Dakota County Groundwater Nitrate Modeling

Prepared for
Dakota County

July 2022

4300 MarketPointe Drive, Suite 200
Minneapolis, MN 55435
952.832.2600
www.barr.com

Dakota County Groundwater Nitrate Modeling

July 2022

Contents

List of Tables

List of Figures

List of Appendices, Attachments, or Exhibits

Certifications

The following certification applies to nitrate leaching rate determination:

I hereby certify that this plan, specification, or report was prepared by me or under my direct supervision and that I am a duly licensed Professional Engineer under the laws of the state of Minnesota.

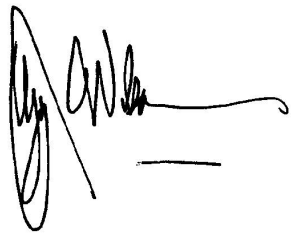

Greg Wilson
PE #: 25782 7/19/2022

The following certification applies to groundwater modeling:

I hereby certify that this plan, document, or report was prepared by me or under my direct supervision and that I am a duly licensed Professional Geologist under the laws of the state of Minnesota.

Evan Christianson
PG #: 51379 Date 7/19/2022

Evan G
Christianson

Digitally signed by Evan G Christianson
Date: 2022.07.19 12:57:59 -05'00'

Abbreviations

AL	Alfalfa
BMP	Best Management Practice
CDL	Cropland Data Layer
CO	Corn
DWSMA	Drinking Water Supply Management Area
lbs	Pounds
MDA	Minnesota Department of Agriculture
MnDNR	Minnesota Department of Natural Resources
MPARS	MnDNR Permitting and Reporting System
MWI	Minnesota Well Index
NASS	National Agricultural Statistics Services
NRCS	Natural Resources Conservation Service
OT	Other (including dry beans, wheat, potatoes, oats, rye, millet, barley, etc.)
PA	Pasture
PE	Peas
SB	Soybeans
SSURGO	Soil Survey Geographic Databases
SWB	Soil Water Balance model
USDA	United States Department of Agriculture

1 Introduction

Groundwater nitrate concentrations in some areas of Dakota County exceed the drinking water standard of 10 mg/L. The Minnesota Department of Agriculture (MDA) has developed modeling to estimate nitrate leaching losses to groundwater under current crop practices that are applicable to the Hastings Drinking Water Supply Management Area (DWSMA).

Dakota County retained Barr Engineering (Barr) to develop and calibrate a groundwater nitrate model of rural portions of the county. The objective was to develop a tool that can be used to account for the current groundwater nitrate load and identify the nitrate-load reduction necessary to achieve a nitrate concentration of 10 mg/L or less on a township level.

Barr previously developed a sub-regional MODFLOW model for Dakota County based on Metro Model 3 (see Section 3). This sub-regional model was combined with the MT3D-USGS (Bedekar et. al., 2016) groundwater transport code to simulate nitrate fate and transport in Dakota County. Nitrate leaching loss rates for current crop practices obtained from the MDA and soil and land cover information were used to inform the modeling.

2 Nitrate Leaching Rates

During the past year, MDA has been actively developing modeling to estimate nitrate leaching losses to groundwater under current crop practices that are applicable to the Hastings DWSMA. MDA has also been using its modeling to run scenarios and analyses to estimate nitrate leaching loss reductions after implementation of various nitrogen best management practices (BMPs).

This section describes how MDA's nitrate leaching estimates within the Hastings DWSMA were utilized and subsequently applied for nitrate leaching loss estimates to groundwater for each of the unique land cover, soils, irrigation, and agricultural management combinations throughout the County.

2.1 Summary of MDA Modeling Results

Several meetings and calls were held with MDA and County staff to better understand the nitrate leaching modeling results, including the assumptions and representativeness for current cropland management within the DWSMA. MDA provided the results of the nitrate leaching modeling for all their modeling scenarios, which included current average nitrate leaching (expressed as nitrogen) estimates based on varying combinations of the following factors:

- Nitrogen fertilizer application methods/rates for corn and soybean crops
- Crop rotation (corn-soybeans, continuous corn)
- Water management (irrigated, non-irrigated)
- Soil series (based on NRCS-USDA SSURGO database)
- Use of cover crops
- Use of perennial land cover.

Based on current cropland management within the DWSMA, MDA indicated that 3 and 4 percent, respectively, of the irrigated and non-irrigated corn and soybean cropland is using cover crops. As a result, the average MDA nitrate leaching estimates for each scenario were weighted based on the relative cover crop areas for irrigated and non-irrigated corn and soybean cropland. MDA's nitrate leaching model results also included the following soil characteristics, averaged based on the depths of each soil layer, that could be paired with the weighted average nitrate leaching estimate for each scenario:

- Texture classification
- Percent sand
- Percent silt
- Percent organic carbon
- Water content, field capacity
- Saturated hydraulic conductivity

All the above soil characteristics, except for percent organic carbon, were obtained from the SSURGO database. MDA estimated percent organic carbon based on percent organic matter, obtained from the SSURGO database, and the following standard conversion formula:

Percent organic carbon = (percent soil organic matter)/1.72

Based on the MDA modeling, there were 16 unique SSURGO soil series areas located within the DWSMA. Since there are several additional SSURGO soil series areas located outside of the DWSMA that would not have been included in the MDA modeling, statistical box plots or regression analyses were developed to evaluate whether the weighted average nitrate leaching estimates for each scenario could be predicted by any one of the six soil characteristics (described above) for each of the following crop rotation and water management combinations:

- Corn-soybeans, irrigated
- Corn-soybeans, non-irrigated
- Continuous corn, irrigated
- Continuous corn, non-irrigated

Analysis of the statistical box plots and regressions indicated that percent organic carbon was the only soil characteristic that had a strong relationship with MDA's weighted average nitrate leaching estimates for each crop rotation and water management combinations. None of the soil characteristics were strong predictors of nitrate leaching. Figure 2-1 shows the relationship between nitrate leaching and percent organic carbon for the irrigated, corn-soybean rotation. Figure 2-2 shows the relationship between nitrate leaching and percent organic carbon for the non-irrigated, corn-soybean rotation. Figure 2-3 shows the relationship between nitrate leaching and percent organic carbon for the irrigated, continuous corn rotation. Figure 2-4 shows the relationship between nitrate leaching and percent organic carbon for the non-irrigated, continuous corn rotation. Linear regressions provided the best fit to the nitrate leaching data in all four figures. The results show that nitrate leaching rates are higher for irrigated cropland than for non-irrigated cropland.

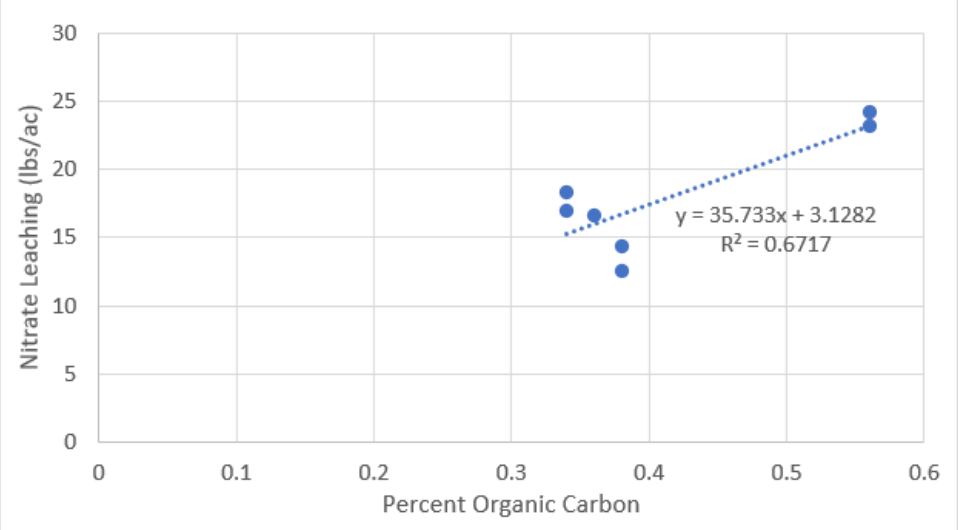

Figure 2-1 Nitrate Leaching Rate and Percent Organic Carbon Relationship—Irrigated, Corn-Soybean Rotation

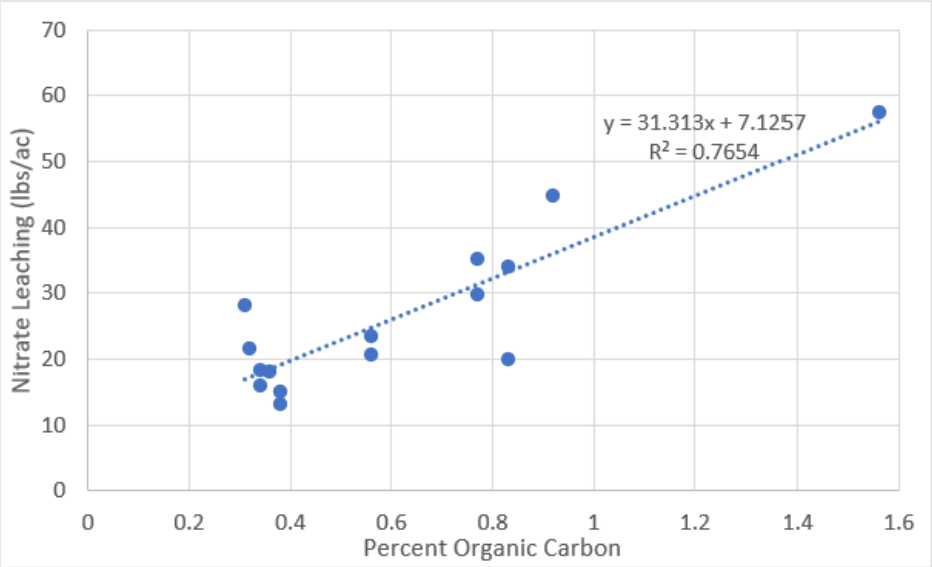

Figure 2-2 **Nitrate Leaching Rate and Percent Organic Carbon Relationship—Non-Irrigated, Corn-Soybean Rotation**

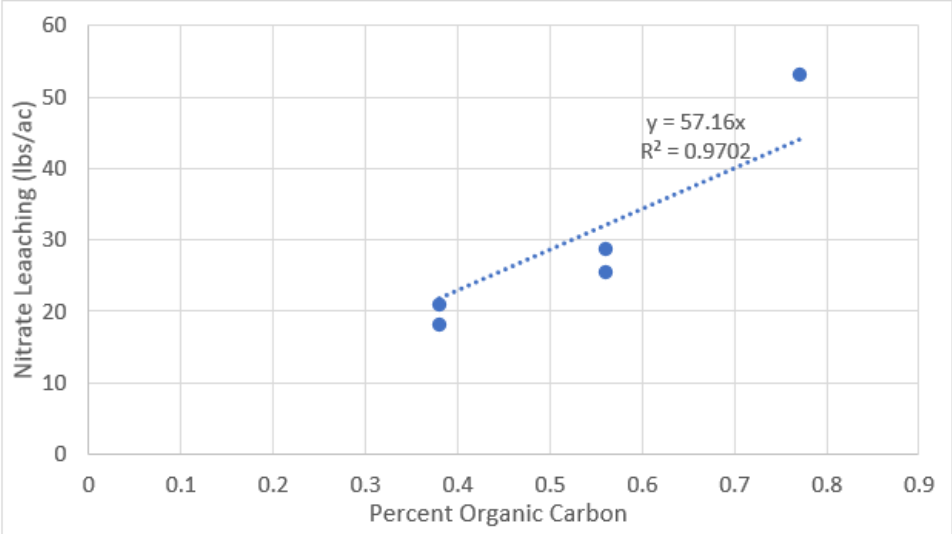

Figure 2-3 **Nitrate Leaching Rate and Percent Organic Carbon Relationship—Irrigated, Continuous Corn Rotation**

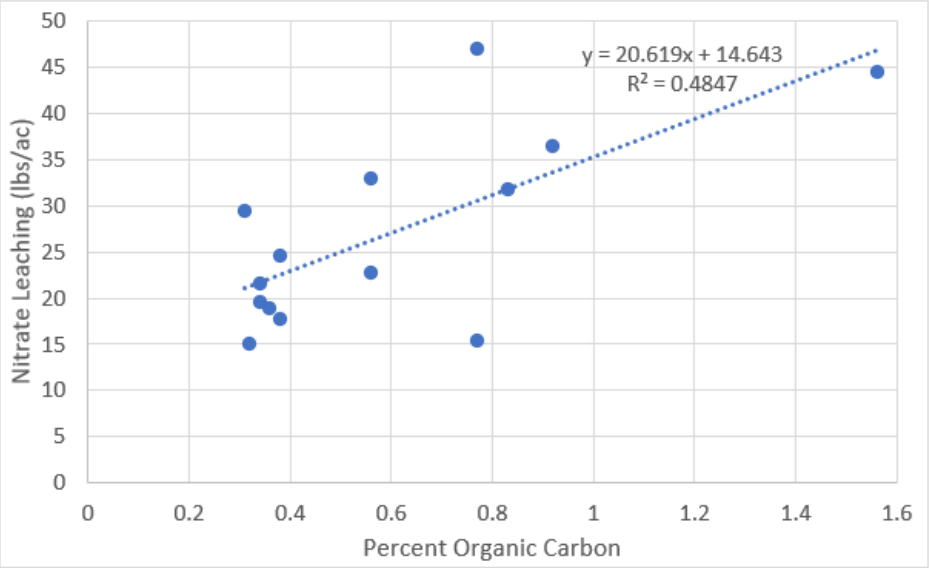

Figure 2-4 **Nitrate Leaching Rate and Percent Organic Carbon Relationship—Non-Irrigated, Continuous Corn Rotation**

2.2 County-Wide Application of Nitrate Leaching Estimates

The United States Department of Agriculture (USDA), National Agricultural Statistics Service (NASS) Cropland Data Layer (CDL) is a raster, geo-referenced, crop-specific land cover data layer that is produced each year. Five years of the NASS USDA CDL datasets for Minnesota, from 2016 through 2020, were obtained and intersected in GIS to develop a data layer with crop rotations throughout Dakota County. It is noted that the CDL datasets were used only to distinguish annual changes to agricultural land cover types and were not used to inventory developed or natural land covers, nor was it used to account for water surface areas. The crop rotation data layer was subsequently intersected with the Dakota radial irrigator coverage in GIS to distinguish crop rotation areas that are irrigated from the non-irrigated areas for each of the respective crop rotations.

Table 2-1 shows the irrigated and non-irrigated acreage associated with each crop rotation category from the GIS intersections. Since MDA had not modeled nitrate leaching for pasture or other miscellaneous crops (such as alfalfa, pasture, peas, dry beans, wheat, potatoes, oats, rye, millet, barley, etc.), Table 2-1 also shows how each crop rotation category was assigned a crop rotation that corresponds with MDA's nitrate leaching estimates. Nitrate leaching estimates associated with pasture, alfalfa and turf land covers were adjusted during groundwater transport model calibration, while nitrate leaching from woodland and other natural areas was simulated with the perennial nitrate leaching rates estimated by MDA.

Table 2-1 Irrigated and Non-Irrigated Agricultural Acreage by Crop Rotation

Rotation	Non-Irrigated (acres)	Irrigated (acres)	Total Acres	Assigned Rotation for Nitrate Leaching Estimates
AL_5	573	22	595	Calibrate
CO_5	5,876	6,211	12,087	C-C
CO_AL	3,233	855	4,089	C-SB
CO_AL_OT	389	116	505	C-SB
CO_OT	755	1,819	2,574	C-C
CO_PE	1,507	4,857	6,365	C-C
CO_PE_AL	459	366	824	C-SB
CO_PE_OT	917	3,066	3,984	C-C
CO_SB	77,939	25,175	103,115	C-SB
CO_SB_AL	5,315	1,735	7,051	C-SB
CO_SB_OT	5,017	3,811	8,829	C-SB
CO_SB_PE	2,490	4,947	7,437	C-SB
OT_5	1		1	C-SB
PA_5	25,834	315	26,149	Calibrate
PE_AL	80	86	166	C-SB
PE_OT	127	17	143	C-SB
SB_5	397	45	442	C-SB
SB_AL	1,727	143	1,870	C-SB
SB_OT	1,473	245	1,718	C-SB
SB_PE_AL	97	26	123	C-SB
TOTALS	**134,207**	**53,859**	**188,066**	

Note(s):

AL – Alfalfa
CO – Corn (incl. Sweet Corn)
PA – Pasture
PE – Peas
SB – Soybeans
OT – Other (incl. Dry Beans, Wheat, Potatoes, Oats, Rye, Millet, Barley, etc.)
_5 – 5 years with no rotation

A data layer containing the assigned rotations and water management (consistent with that shown in Table 2-1) was intersected with the SSURGO soil series layer in GIS to generate the unique identifiers (crop rotation—water management—soil series combinations) that were subsequently used to calculate the weighted nitrate leaching rate (based either on MDA's direct estimates, Figures 2-1 through 2-4, or an assumption that can be used for calibration) for each 125-meter grid cell, county-wide. The final nitrate leaching rates used in the groundwater modeling were capped at 100 lbs/ac for instances where the percent organic carbon content resulted in calculated nitrate leaching rates that exceeded that threshold.

3 Groundwater Flow Model Development

In 2017, Barr Engineering Co. constructed and calibrated a MODFLOW-based sub-regional groundwater flow model derived from the Twin Cities Metropolitan Area Regional Groundwater Flow Model (Metro Model 3, Metropolitan Council, 2014), for the Dakota County area. The sub-regional model, hereafter referred to as the *local model*, includes finer grid resolution than Metro Model 3 in order to better simulate groundwater flow across Dakota County. This local flow-model was reviewed and deemed the best available tool to simulate groundwater flow for this project. The local flow model was combined with the groundwater transport code MT3D-USGS to simulate nitrate fate and transport (see Section 4). Documentation of the groundwater flow model construction and calibration is provided below for reference. For this project, no additional adjustment or calibrations were made to the local groundwater flow model. The only updates were the inclusion of nitrate fate and transport with the MT3D-USGS code.

The construction and calibration of the local model followed similar procedures to those used in the construction of the Metro Model 3. Specific changes and updates made to the local model are described in the following sections. The hydrogeologic conceptual model is the same for both the local and regional models and is described in Metropolitan Council (2014). Where applicable, descriptions of model design, parameter selection, and model calibration from the Metro Model 3 report (Metropolitan Council, 2014) are included within this document for clarification. However, the reader is encouraged to review the Metro Model 3 report for additional background and description.

3.1.1 Local Model Domain and Discretization

Figure 3-1 shows the domain of the local model relative to the Metro Model 3 domain. The local model domain covers 1,409 square miles and encompasses all of Dakota County and portions of Hennepin, Ramsey, Washington, Scott, Goodhue, and Rice Counties in Minnesota. The local model was discretized on a 125-meter square grid. This represents a 16x refinement of Metro Model 3; i.e., there are sixteen local model cells for every one 500-m square Metro Model 3 cell.

The bottom of the local model is the base of the Jordan Sandstone and the top is the ground surface. Bottom elevations for the base of the model were extracted from the bottom of layer 4 of the Metro Model 3 (which generally represents the Jordan Sandstone within the local model domain). Lidar data were used to define the top of layer 1.

The uppermost layer of Metro Model 3 was subdivided into two separate layers for the local model, resulting in a total of five model layers in the local model (Figure 3-2). The additional layer allows for an explicit representation of the combined Decorah Shale/Platteville Formation/Glenwood Formation, an important confining unit and the uppermost bedrock in portions of Dakota County. In Metro Model 3 the Decorah Shale/Platteville Formation/Glenwood Formation is lumped with Quaternary sediments into a bulk effective hydraulic conductivity. The additional layer in the local model also allows for a finer resolution of the shallow Quaternary stratigraphy.

3.1.2 Hydrostratigraphic Units

Hydrostratigraphic unit extents mapped by Mossler (2013) were updated on the refined grid. The local model layers generally represent the following hydrostratigraphic units:

- Layer 1: Quaternary sediments
- Layer 2: Decorah Shale, Platteville Formation, and Glenwood Formation if present, otherwise Quaternary sediments
- Layer 3: St. Peter Sandstone if present, otherwise Quaternary sediments
- Layer 4: Prairie du Chien Group if present, otherwise Quaternary sediments
- Layer 5: Jordan Sandstone if present, otherwise Quaternary sediments

Due to faulting in Washington and Dakota Counties, bedrock units may be present in shallower layers than those listed above (e.g., Prairie du Chien in layer 3 instead of layer 4). In addition, in the faulted regions some cells represent hydrostratigraphic units that are usually found below the base of the local model (e.g., St. Lawrence Formation, Tunnel City Group, Wonewoc Sandstone). Boundaries of the faulted regions were left unchanged from the Metro Model 3. Figure 3-2 shows a cross-section through the model and Figure 3-3 shows maps of the local model hydrostratigraphic unit extents for model layers 2-5.

The refined model grid allows for full use of the mapping of Quaternary sediment material types conducted by Tipping (2011). Tipping mapped materials to a 250-meter square grid in the horizontal direction with horizontal slices every 6.1 meters (20 feet) in the vertical direction. The MODFLOW grid of the local model is designed so that each of Tipping's 250-meter square grids representing different material types is represented by four MODFLOW cells.

3.1.3 External Boundary Conditions

The external perimeter boundaries of the local model, including the bottom, are simulated using general head boundaries. The head at each perimeter boundary cell is defined using Darcy-planar interpolation of the Metro Model 3 heads. The conductance of the general head boundaries is equivalent to the conductance of two prisms in a series; referred to as the ghost-node conductance in Mehl and Hill (2013). Essentially, along the boundary of the local model the neighboring Metro Model 3 cell geometry and hydraulic conductivity is used to define one conductance and the cell geometry and hydraulic conductivity of the local model cell is used to define a second conductance. These two conductance values are then combined in series to define the conductance of the general head boundary cell. For more detail, see Mehl and Hill (2013, pg. 11).

3.1.4 Surface Water Features

The same rivers, streams, and lakes are simulated in both Metro Model 3 and the local model using the river boundary package. Only perennial portions of the rivers and streams, as defined in the National Hydrological Dataset, were included. GIS shapefiles developed for Metro Model 3 were used to define the extent and stage of each river boundary cell (Figure 3-4). The much finer grid of the local model compared to Metro Model 3 allows for more accurate representation of the geometry of individual surface-water features.

3.1.5 Precipitation Derived Infiltration

The Soil Water Balance (SWB) model (Dripps and Bradbury, 2007) developed for Metro Model 3 (Metropolitan Council, 2012a) was used in conjunction with the Unsaturated-Zone Flow (UZF) package in MODFLOW for implementing precipitation-derived infiltration in the local model. The SWB model output was remapped from the 90 meter by 90 meter SWB grid to the 125 meter by 125 meter local model grid using an area-weighted average. The SWB model output defines the initial distribution of precipitation-derived infiltration across the local model domain.

3.1.6 High-Capacity Pumping

High-capacity wells in both the local model and Metro Model 3 were updated with data from the Minnesota Department of Natural Resources (MnDNR) Permitting and Reporting System (MPARS) database. For the purposes of the steady-state calibration, the pumping rates used in both Metro Model 3 and the local model were 2006-2015 averages.

It is not appropriate to include all pumping records from the MPARS database in a groundwater model. The following pumping data were not used:

- All appropriations with a "Surface Water" resource code **except** those records with use types of "Mine Dewatering", "Quarry Dewatering", and "Sand/Gravel Pit Dewatering." These exceptions, while classified as "Surface Water", likely represent groundwater pumping.
- Temporary groundwater pumping (e.g., construction dewatering, appropriations covered under general permit 1997-0005).
- Any groundwater appropriation with insufficient information in both the MPARS and Minnesota Well Index (MWI) databases (e.g., aquifer name, well depth) to determine the appropriate model layer(s) in which to specify the pumping.

The second and third bullets above result in the exclusion of approximately 2% of the total reported groundwater pumping within the Metro Model 3 domain.

3.2 Groundwater Flow Model Calibration

Model calibration involves adjusting model parameters until the model results acceptably match observations such as measured water levels and estimated stream baseflow. The local model was calibrated through a series of automated inverse optimization procedures using the model-independent parameter estimating software BEOPEST (Version 13.3; Doherty, 2010b). Optimization in this sense is defined as minimizing the differences, or residuals, between simulated results and observations. The objective function that is minimized by BEOPEST is the sum of squared weighted residuals for all calibration targets. The square of the residual is used because some residuals are negative and some are positive. BEOPEST is part of the PEST family of optimization software (Doherty 2010a; Doherty, 2013) and uses exactly the same optimization algorithms as PEST. The main difference between the two is that BEOPEST offers much greater flexibility in handling parallel run management (calibration on many machines or processors at once). Throughout this document PEST and BEOPEST may be referred to interchangeably as they both refer to the same algorithms and methods.

The overall process of the calibration procedure employed for this study was as follows:

1. The model was constructed.
2. Calibration targets were chosen. Weights were assigned to the targets based on factors such as the quality of the data (e.g., greater weight on more accurate measurements).
3. Parameters that were allowed to vary during the calibration process were chosen, along with the ranges over which parameters were allowed to vary.
4. PEST was run.
5. The results of the PEST optimization were evaluated and adjustments were made to the PEST input file if necessary. Examples of such adjustments include: changing the weights to put more emphasis on matching certain targets, revising the upper and/or lower parameter bounds, and fixing the values of parameters identified by PEST as insensitive in order to reduce the number of model runs.
6. Steps 4-5 were repeated numerous times to improve the optimization.

The "best" parameter set determined by a PEST optimization run is not unique; that is, other combinations of parameters may produce nearly identical results. This issue can be minimized by using more (and more varied) types of targets during the calibration (Hill and Tiedeman, 2007) and by placing constraints on the range over which a parameter can vary (i.e., upper and lower bounds). Both of these remedies were implemented for this project. Section 3.2.1 below discusses the numbers and types of targets used. Tikhonov regularization constraints (Doherty, 2003; Fienen et al, 2009; Tikhonov, 1963) were implemented to constrain the parameter ranges and avoid the tendency of insensitive parameters to move toward extreme values to achieve minimal progress in lowering the objective function.

3.2.1 Calibration Targets

Calibration targets for the local model are similar to those used for calibration of Metro Model 3. However, where possible, they were updated with new data. For example, available data collected after 2011 were included.

Calibration targets included the following:

- 73 average 2006-2016 water levels from MnDNR observation wells
- 807 water levels from the MWI database measured in 2006 or later
- 12,834 water levels from the MWI database measured before 2006
- 8 baseflow discharge estimates for stream, or portions of streams, within the local model
- 53 transmissivity estimates from pumping tests conducted at high-capacity wells within the local model
- 7 flow direction targets defined by the axes of mapped plumes of groundwater contamination (Metropolitan Council, 2012b). Modeled flow directions for each target were calculated by using three simulated hydraulic head values around the axis of the target to solve a three-point problem (Fienen, 2005).

3.2.2 Parameters

3.2.2.1 Bedrock Hydraulic Conductivity

As described in Metropolitan Council (2014) and in detail by Runkel and others (2003), the bulk hydraulic conductivity of bedrock aquifers and aquitards in southeastern Minnesota is controlled by both primary hydraulic conductivity (matrix permeability) and secondary hydraulic conductivity (systematic fractures, dissolution features, and nonsystematic fractures). To capture these two main components of the bulk hydraulic conductivity, the same methods as used for Metro Model 3, and described below, were employed for calibration of the local model.

The primary hydraulic conductivity (K_{px}) and vertical anisotropy ($\frac{K_{bx}}{K_{bz}}$) were estimated using pilot points (Doherty and others, 2010). Ordinary kriging was used to interpolate between pilot points for each hydrostratigraphic unit. Twenty-six pilot points were distributed evenly across the local model domain to allow for relatively smooth interpolated distributions. Additionally, pilot points were set at fixed values equal to the value used in Metro Model 3 at each location along the perimeter of the local model. This allows the hydraulic conductivity to be adjusted within the local model and transition smoothly, via interpolation, to the value used by Metro Model 3 at the edge of the local grid.

A depth-dependent function was used to increase the hydraulic conductivity values for individual units where they are near the top of bedrock surface. Features controlling secondary hydraulic conductivity are known to be present at all depths but are most prevalent within 200 feet of the top of bedrock surface (Runkel and others, 2003).

The depth-dependent function used is shown in equation 1 below:

$$D = C * \left(10^{-\lambda d}\right) + 1 \qquad \textit{(Eqn. 1)}$$

where:

D = scaling factor used to determine total hydraulic conductivity
C = constant used to control the max value of *D*
λ = constant used to control max depth (*d*) at which *D* is greater than 1
d = depth of unit below bedrock surface

To determine the bulk hydraulic conductivity for input to MODFLOW, equation 2 and equation 3 were used on a cell-by-cell basis for horizontal and vertical hydraulic conductivity, respectively.

$$K_{bx} = K_{px} * D \qquad \textit{(Eqn. 2)}$$

$$K_{bz} = \frac{K_{bx}}{K_{bz}} * K_{bx} \qquad \textit{(Eqn. 3)}$$

where:

K_{bx} = bulk horizontal hydraulic conductivity used as input for MODFLOW

K_{bz} = bulk vertical hydraulic conductivity used as input for MODFLOW

K_{px} = primary horizontal hydraulic conductivity

$(\frac{K_{bx}}{K_{bz}})$ = vertical anisotropy ratio

D = scaling factor determined with Eqn. 1

For model calibration, values of C and λ, used in Equation 1, for each hydrostratigraphic unit were set as adjustable parameters.

3.2.2.2 Quaternary Hydraulic Conductivity

The same methods as used for Metro Model 3, and described below, were employed to calculate effective horizontal and vertical hydraulic conductivities of the Quaternary sediments in the local model. Effective hydraulic conductivities were calculated for each model cell based on material type and thickness (e.g., sand, clay) within each model cell. The type, extent, and thickness of Quaternary sediments in the 11-county metropolitan area were determined from mapping conducted by Tipping (2011).

The material types classified by Tipping (2011) are mapped as a matrix of points spaced 250 meters (820 feet) apart in the horizontal direction and 6.1 meters (20 feet) apart in the vertical direction. The point data set from Tipping (2011) was converted to a series of raster grids, each representing material types along a single elevation (each elevation raster was spaced 20 feet apart). In order to distinguish between MODFLOW model cells and the material-type raster cells, the material-type raster cells are referred to as material type "voxels" throughout the rest of this section.

The MODFLOW grid was constructed such that four of the model cells (which are 125 m by 125 m in size) lie within each material-type voxel (each representing 250 m by 250 m). This is a difference from Metro Model 3, for which four material-type voxels were contained within each 500 m by 500 m model cell.

A series of external processing scripts was developed to determine the thickness of each material type and to calculate the effective horizontal and vertical hydraulic conductivities for each material-type voxel that intersects a MODFLOW cell. The general process is as follows:

1) The thicknesses of each material type that intersects a MODFLOW cell ($b_{i,j}$) were determined using the bottom of the MODFLOW cell and the minimum of either the top of the MODFLOW cell or the water table (only saturated thicknesses were used to determine the effective hydraulic conductivities). The water-table elevations used for these calculations are based on the regional water-table surface as developed by Barr Engineering (2010).
2) The horizontal hydraulic conductivity value applied to the MODFLOW cells is the effective horizontal hydraulic conductivity calculated from the horizontal hydraulic conductivities for each material type voxel $(Kx)_{i,j}$ using equation 4 (Anderson and Woessner, 1992).

$$(K_x)_{i,j} = \sum_{g=1}^{m} \frac{Kx_{i,j,g} b_{i,j,g}}{B_{i,j}}$$ (*Eqn. 4*)

$$B_{i,j} = \sum_{g=1}^{m} b_{i,j,g}$$ (*Eqn. 5*)

where:

$B_{i,j}$ = the total saturated thickness of a model cell

$b_{i,j,g}$ = the thickness of an individual material type

$Kx_{i,j,g}$ = the horizontal hydraulic conductivity of an individual material type

m = the total number of materials that intersect a MODFLOW cell

3) The vertical hydraulic conductivity value applied to the MODFLOW cells is the effective vertical hydraulic conductivity calculated from the vertical hydraulic conductivities for each material type voxel $(Kz)_{i,j}$ using equation 6 (Anderson and Woessner, 1992).

$$(K_z)_{i,j} = \frac{B_{i,j}}{\sum_{g=1}^{m} \frac{b_{i,j,g}}{Kz_{i,j,g}}}$$ (*Eqn. 6*)

where:

$B_{i,j}$ = the thickness of a model cell

$b_{i,j,g}$ = the thickness of an individual material type

$Kz_{i,j,g}$ = the vertical hydraulic conductivity of an individual material type

m = the total number of materials that intersect a MODFLOW cell

3.2.2.3 Lakebed and riverbed conductance

The conductance of river boundary cells is expressed as:

$$C = \frac{KA}{M}$$ *(Eqn. 7)*

where:

C = the conductance of river boundary for cell

K = the hydraulic conductivity of the riverbed or lakebed

A = the area of the river or lake that intersects the cell

M = the thickness of the riverbed or lakebed sediments

For purposes of model calibration, the hydraulic conductivity of the lake/riverbed sediments was used as an adjustable parameter for calculating river cell conductance; the thickness of the riverbed or lakebed sediments was assumed to be equal to one meter. Lakes were categorized into 14 different groups based on surficial geology (Hobbs and Goebel, 1982). The hydraulic conductivity of lakebed sediments for each group was adjusted as part of the calibration process. The hydraulic conductivity of riverbed sediments for each major river was adjusted as part of the calibration process. Each river was subdivided into several reaches; a total of 77 river reach segments were used (Figure 3-4).

3.2.2.4 Precipitation-Derived Infiltration

Precipitation-derived infiltration was parameterized in the same way as was done in Metro Model 3. Sensitivity analysis of the SWB input parameters and uncertainty analysis of the SWB output as described in Appendix A of Metropolitan Council (2012a) were used to guide how precipitation-derived infiltration could vary during calibration of the local groundwater flow model. Scaling factors were established for each combination of land use and soil type in order to allow precipitation-derived infiltration to vary during calibration of the groundwater flow model while keeping the precipitation-derived infiltration within expected ranges and tied to the uncertainty, which can vary across the model domain.

3.2.3 Groundwater Flow Model Calibration Results

Model fit was evaluated using several different calibration statistics along with visual comparison of measurements to simulated model results. Residuals used in calculating statistics were defined in the same way as calculated by PEST:

$$residual = measured - simulated$$

Calculating residuals as defined above results in somewhat counterintuitive residual signs. Negative residuals indicate that the model-simulated values are greater than measured values and positive residuals indicate that the model-simulated values are less than measured values.

Plots showing measured versus simulated hydraulic-head targets for each target group are shown on Figure 3-5 to Figure 3-7. Table 3-1 below summarizes the calibration statistics for hydraulic-head calibration targets across the different target groups.

Table 3-1 Summary of hydraulic head calibration statistics

Target Group	Residual Mean (m)	Absolute Residual Mean (m)	Root Mean Square Error (RMSE) (m)	Ratio of RMSE to Measurement Range
MN DNR ObWells	-0.29	2.69	4.17	0.04
MWI Pre-2006	-2.31	6.67	10.06	0.07
MWI Post-2006	-0.54	6.76	10.16	0.06

The residual mean measures the average tendency of simulated values to be greater (negative residual mean) or less than (positive residual mean) measured values. The residual mean ranged from -2.31 meters to -0.29 meters for individual head-target groups, indicating that the model tends to simulate slightly higher water levels than measured. The absolute residual mean is the average of the absolute value of the residuals. The absolute residual mean ranged from 2.69 meters to 6.76 meters for individual head-target groups. The root mean square error (RMSE) is the square-root of the average of the squared residuals. RMSE is a model-calibration statistic that is generally more sensitive to outliers than other model-calibration statistics and gives a better sense of the range of residuals. RMSE ranged from 4.17 meters to 10.16 meters for individual head-target groups. RSME is often compared to the ranges in measurements; a small value for the ratio of RMSE to the range of measured values (typically less than 0.1) indicates good overall model fit (Spitz and Moreno, 1996). The ratio of RSME to the range in measurements ranged from 0.04 to 0.07 for individual target groups, indicating that the calculated RMSE is acceptable given the range of measured heads across the model domain.

Water levels fluctuate over time in response to climatic variations and changes in pumping that cannot be explicitly represented in a steady-state model such as the local model in this study. The MnDNR observation well targets take some of this variability into account because these target values were calculated by averaging multiple measurements collected at each well. The MnDNR targets were matched quite well in the model calibration. The calibrated model did not match the MWI head targets as well, but this is to be expected given the lower quality of these data, which are typically single measurements taken immediately after well installation. Section 4.1.1 of Metropolitan Council (2014) discusses in detail the many sources of error in the available water level data.

Measured and simulated baseflow and calculated percent error are presented below in Table 3-2. A plot showing measured vs simulated baseflow is shown on Figure 3-8.

Table 3-2 Summary of measured and simulated baseflow statistics

River Reach	Measured (m^3/day)	Simulated (m^3/day)	Percent Error
Cannon River above Welch, MN	-984,497	-1,207,309	23%
Credit River	-29,775	-31,217	5%
Mississippi River between St. Paul, MN and Hastings, MN	-293,100	-307,610	5%
Minnesota River Between Jordan, MN and Fort Snelling State Park, MN	-1,181,400	-1,170,402	-1%
Nine Mile Creek	-35,720	-37,362	5%
St. Croix River between St. Croix Falls, WI and Mississippi River	-1,545,400	-1,100,263	-29%
Vermillion River upstream of Empire, MN	-117,660	-108305	-8%
Valley Creek	-31,781	-29,616	-7%

As shown in Table 3-2, the modeled baseflows were generally within 10% of the target values, which is considered good agreement given that the targets are estimates based on analysis of streamflow data. Baseflow estimation is challenging for long stream reaches within which significant tributaries join the main stream, and this may explain the higher residuals for the entire Cannon River upstream of Welch, MN and the long St. Croix reach.

The values of transmissivity calculated from pumping tests across the metro area were used as observations (i.e., "measured" transmissivity). During the optimization process, the transmissivities at these pumping test locations were calculated from the values of hydraulic conductivity (multiplied by saturated thickness), which were adjustable parameters at the pilot point locations. The residual (i.e., difference) between the "measured" transmissivity values and the model-calculated values contributed to the overall objective function and PEST attempted to minimize these residuals in the context of the overall optimization process.

Simulated transmissivity at the pumping test locations was typically less than the "measured" transmissivity (Figure 3-9). The mean percent error was -13% and the mean absolute percent error was 32%. This bias may be a result of several factors. Regularization controls on bedrock hydraulic conductivity pilot points and the relatively small number of pilot points used may have hindered the calibration process from achieving a better match with measured transmissivity. Also, "measured" transmissivity values are the products of analytical calculations that employ severely limiting assumptions such as an infinite areal aquifer extent and are themselves subject to considerable uncertainty. "Measured" values may actually be biased high due to inaccurately accounting for leakage in the analysis of aquifer tests and because wells are often completed in the most productive zones of an aquifer.

3.2.4 Estimated Parameter Values

Figures A-1 through A-8 in Appendix A show the final calibrated hydraulic conductivity fields for each bedrock hydrostratigraphic unit. As discussed above in Section 3.2.2.1, the hydraulic conductivity field is interpolated from the individual pilot points shown on the figures and then the depth-dependent function is applied to the interpolated field. Because the depth-dependent function is applied after the interpolation, the hydraulic conductivity values of the individual pilot points shown on the figures do not take the depth-dependent function into account.

Figures A-9 through A-18 in Appendix A show the spatial distribution of calibrated hydraulic conductivity values for Quaternary sediments in each model layer. The mapped values represent effective hydraulic conductivity calculated using methods discussed in 3.2.2.2 from the values of individual Quaternary material types listed below in Table 3-3. These values are within typical ranges for these materials (Freeze and Cherry, 1979).

Table 3-3 Quaternary material hydraulic conductivity values

Quaternary Material Type	Horizontal Hydraulic Conductivity (m/day)	Vertical Hydraulic Conductivity (m/day)
Sand and Gravel	1.4E+01	6.9E+00
Fine Sand	9.6E+00	1.9E+00
Loam to Sandy Loam	2.6E+00	5.1E-01
Loam to Sandy Clay Loam	8.1E-01	1.9E-02
Sandy Silt	2.2E-01	6.9E-03
Loam to Sandy Loam - Deep	1.3E-02	2.4E-05
Loam to Sandy Clay Loam - Deep	1.2E-02	1.2E-04
Loam, Silt Rich; Silt and Clay	1.0E-02	5.9E-04
Loam to Clay Loam	3.3E-04	6.0E-06
Loam, Silt Rich; Silt and Clay - Deep	2.7E-04	1.7E-05
Loam to Clay Loam	9.1E-06	1.8E-06

As discussed in Section 3.1.5, precipitation-derived infiltration, as calculated using the SWB model, was used to define the initial distribution of precipitation-derived infiltration across the entire model domain. Uncertainty analysis of the SWB model results were used to develop scaling factors, or multipliers, for each combination of land use and soil type. The calibrated multipliers are shown below in Table 3-4. The final distribution of precipitation-derived infiltration across the model domain is shown on Figure A-19.

Table 3-3 Precipitation-Derived Infiltration Multipliers

Land Use	A Soils	B Soils	C Soils	D Soils
Open Water	1.00	1.00	1.00	1.00
Low Density Residential	1.20	0.90	1.00	0.69
High Density Residential	1.27	1.09	1.00	1.02
Commercial / Industrial / Transient	1.22	1.99	0.98	0.83
Bare Rock / Sand	1.00	1.00	1.00	1.00
Quarries / Pits	1.00	0.63	1.00	0.86
Deciduous Forest	1.00	1.15	1.00	0.69
Evergreen Forest	1.00	1.00	1.00	1.03
Mixed Forest	1.00	1.00	1.00	1.00
Shrub Land	1.18	1.11	1.00	1.04
Grass / Herbs	1.07	1.00	1.00	0.97
Pastures	1.00	1.00	1.00	0.71
Row Crops	1.00	1.21	1.00	1.25
Urban / Recreational Grass	1.15	1.10	1.00	1.38
Wetlands	1.00	1.00	1.00	0.64

Figure 3-1 Local Model Domain

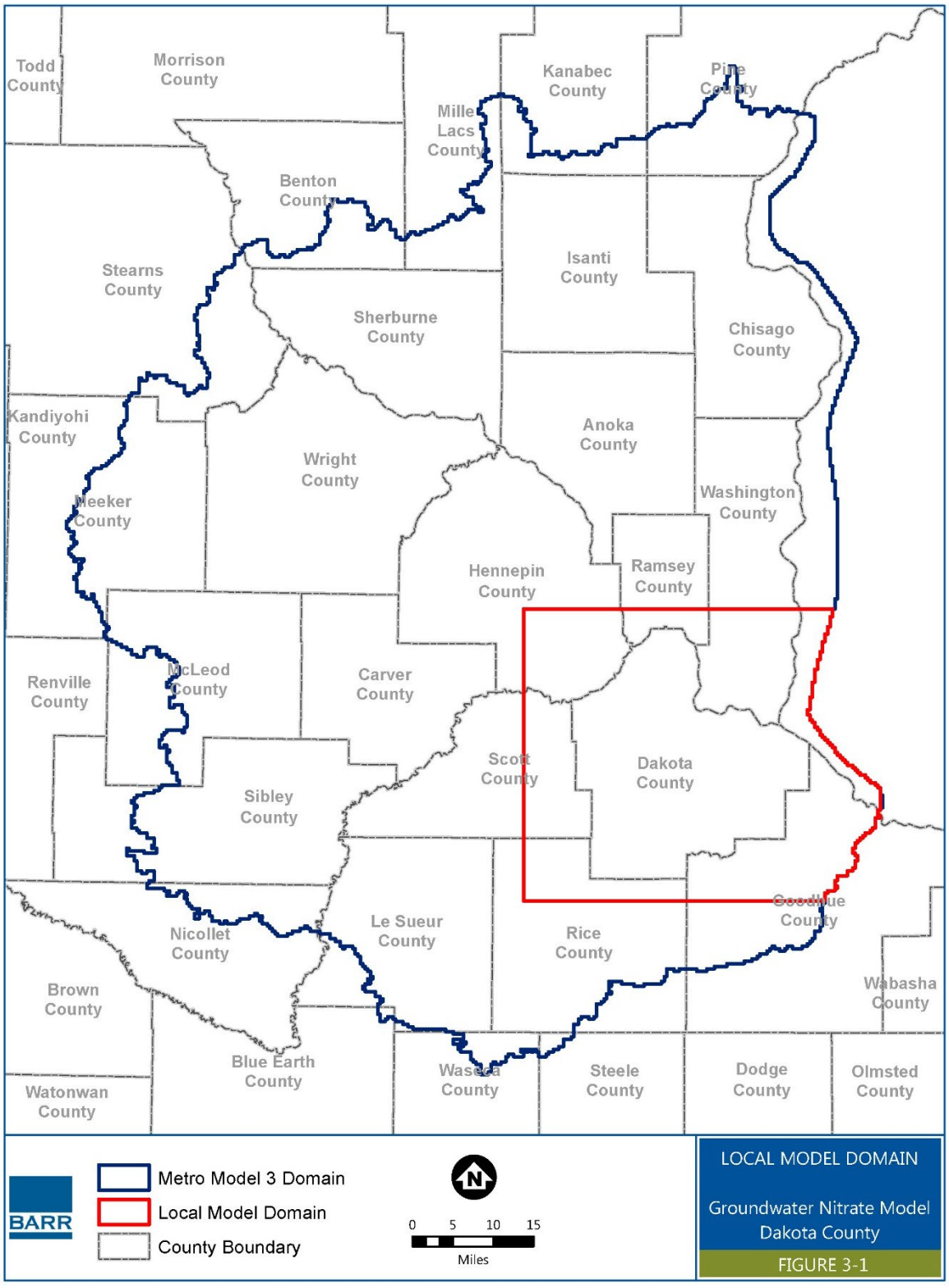

Figure 3-2 Model Cross Section

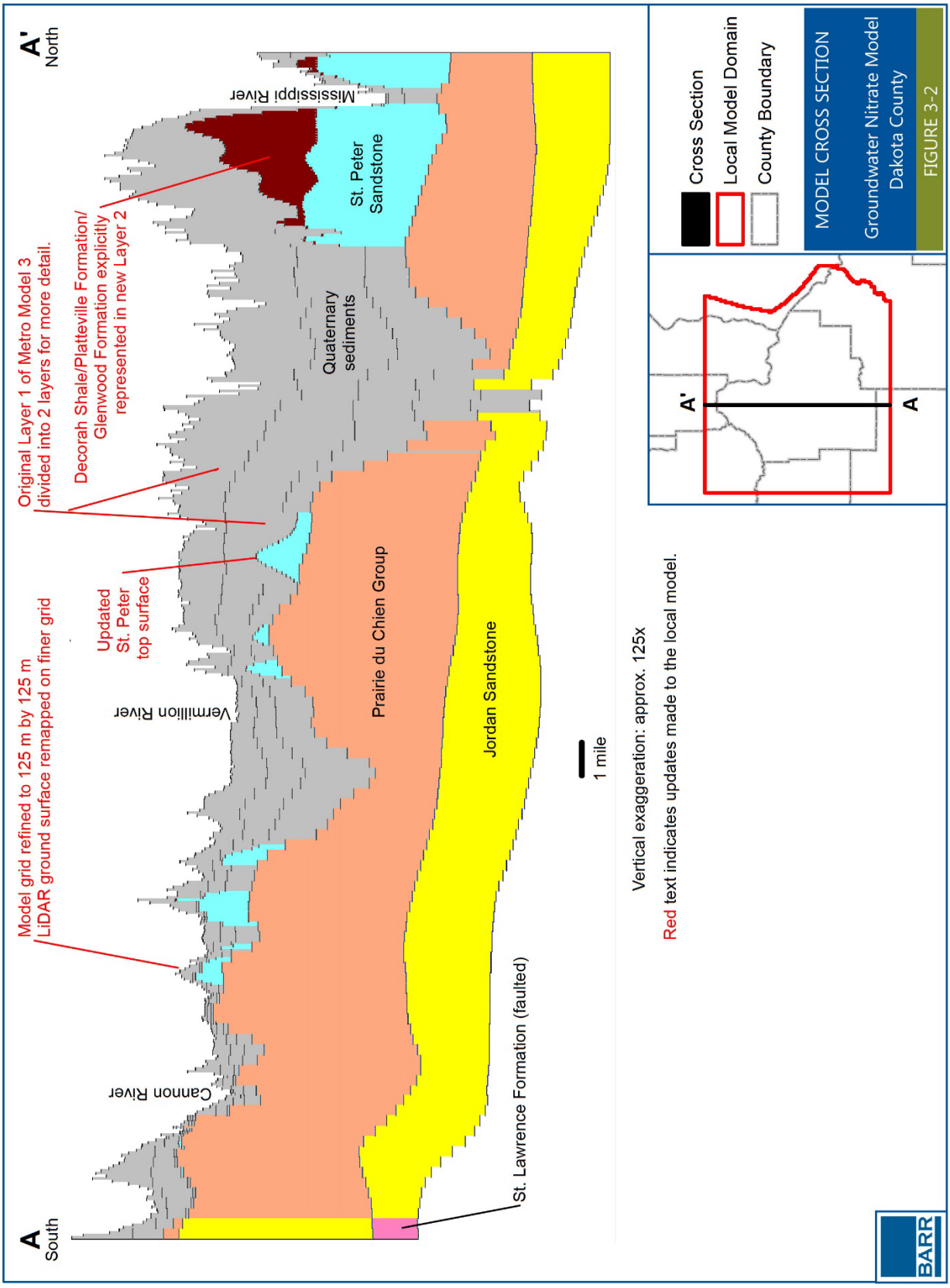

Figure 3-3 Hydrostratigraphic Units

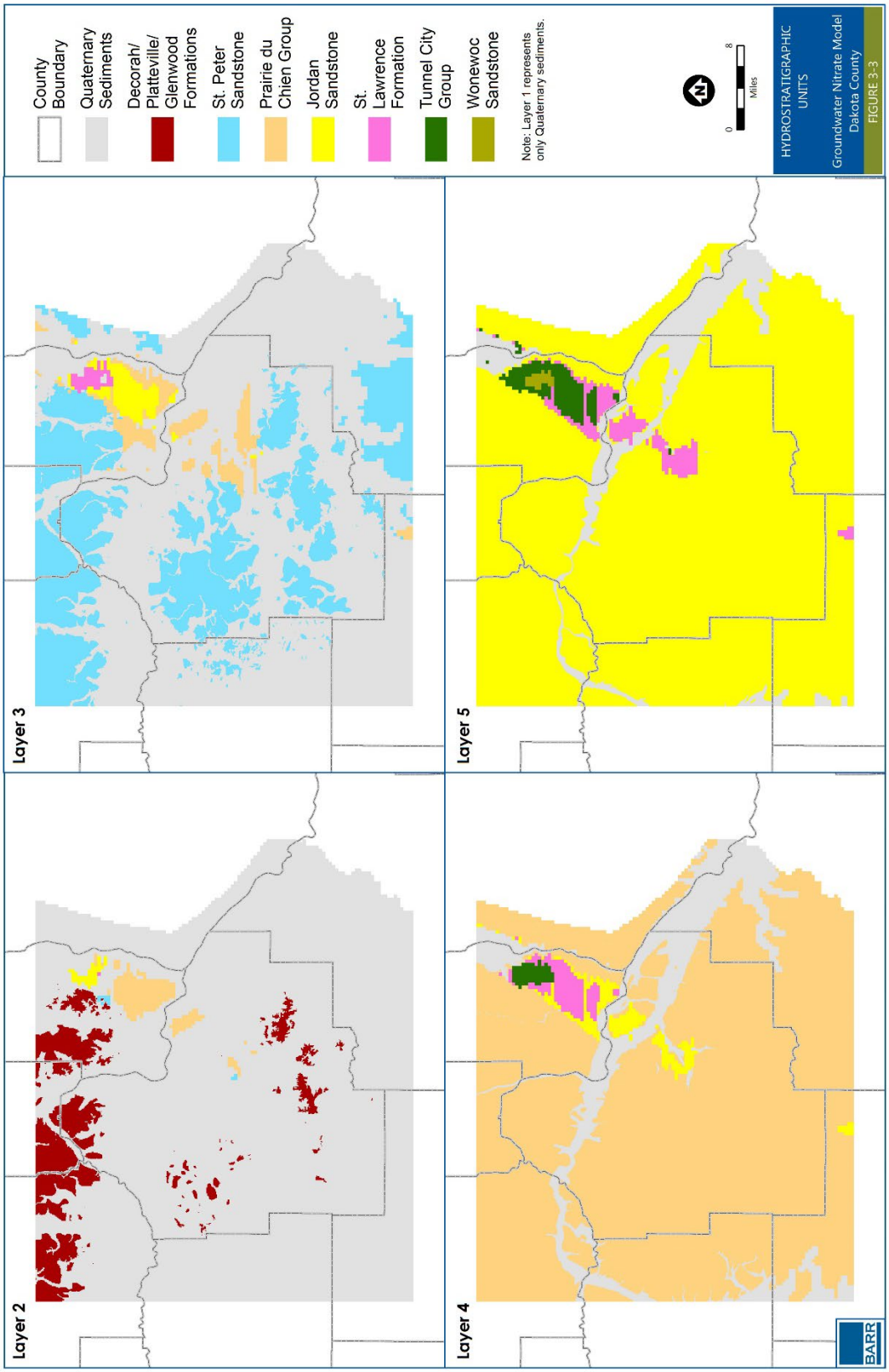

Figure 3-4 Lake and River Reach Conductance Zones

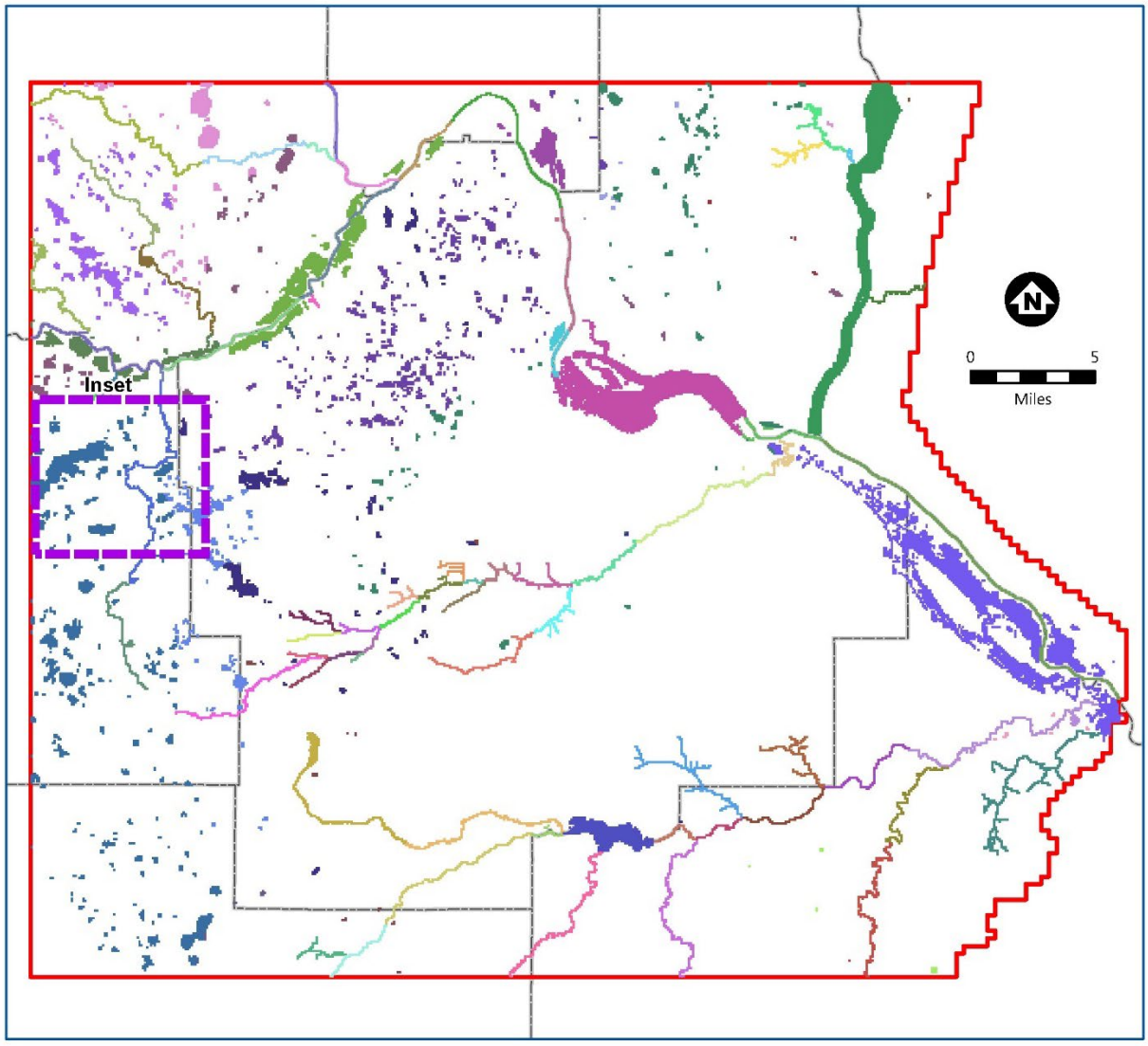

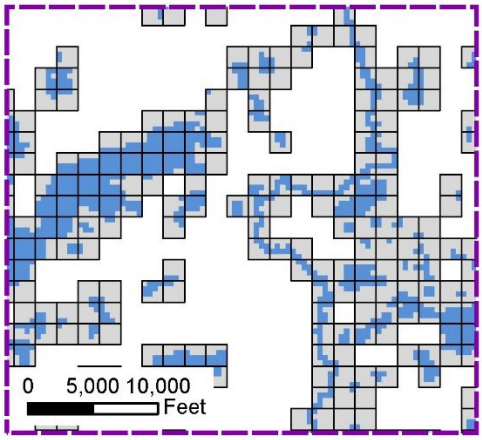

Inset showing the greater detail achieved for representing rivers and lakes with the refined grid of the local model (blue) compared to Metro Model 3 (gray).

BARR

LAKE AND RIVER REACH CONDUCTANCE ZONES

Groundwater Nitrate Model
Dakota County

FIGURE 3-4

Figure 3-5 Measured vs Simulated Hydraulic Heads, Minnesota Well Index, Pre-2006

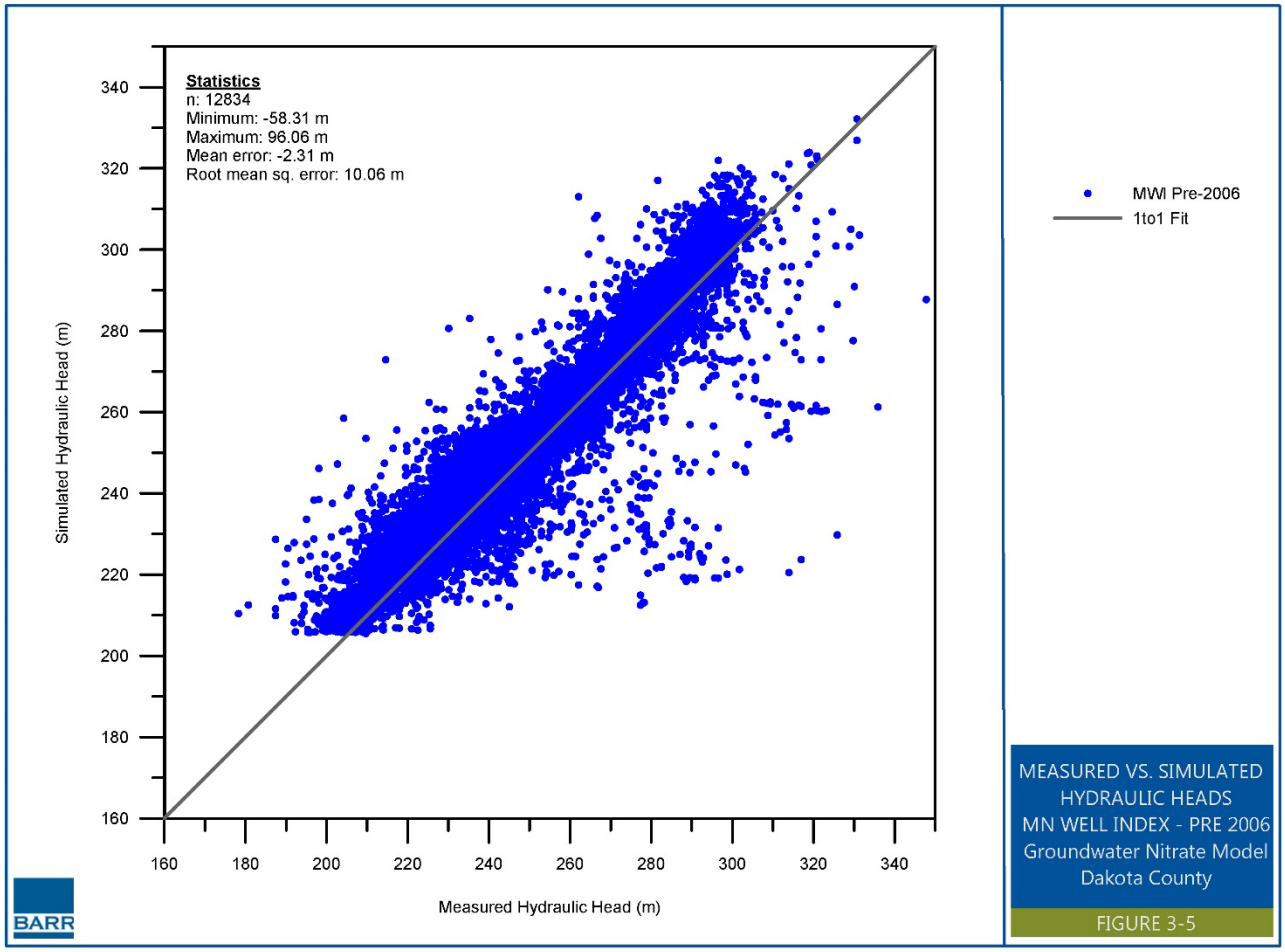

Figure 3-6 Measured vs Simulated Hydraulic Heads, Minnesota Well Index, Post-2006

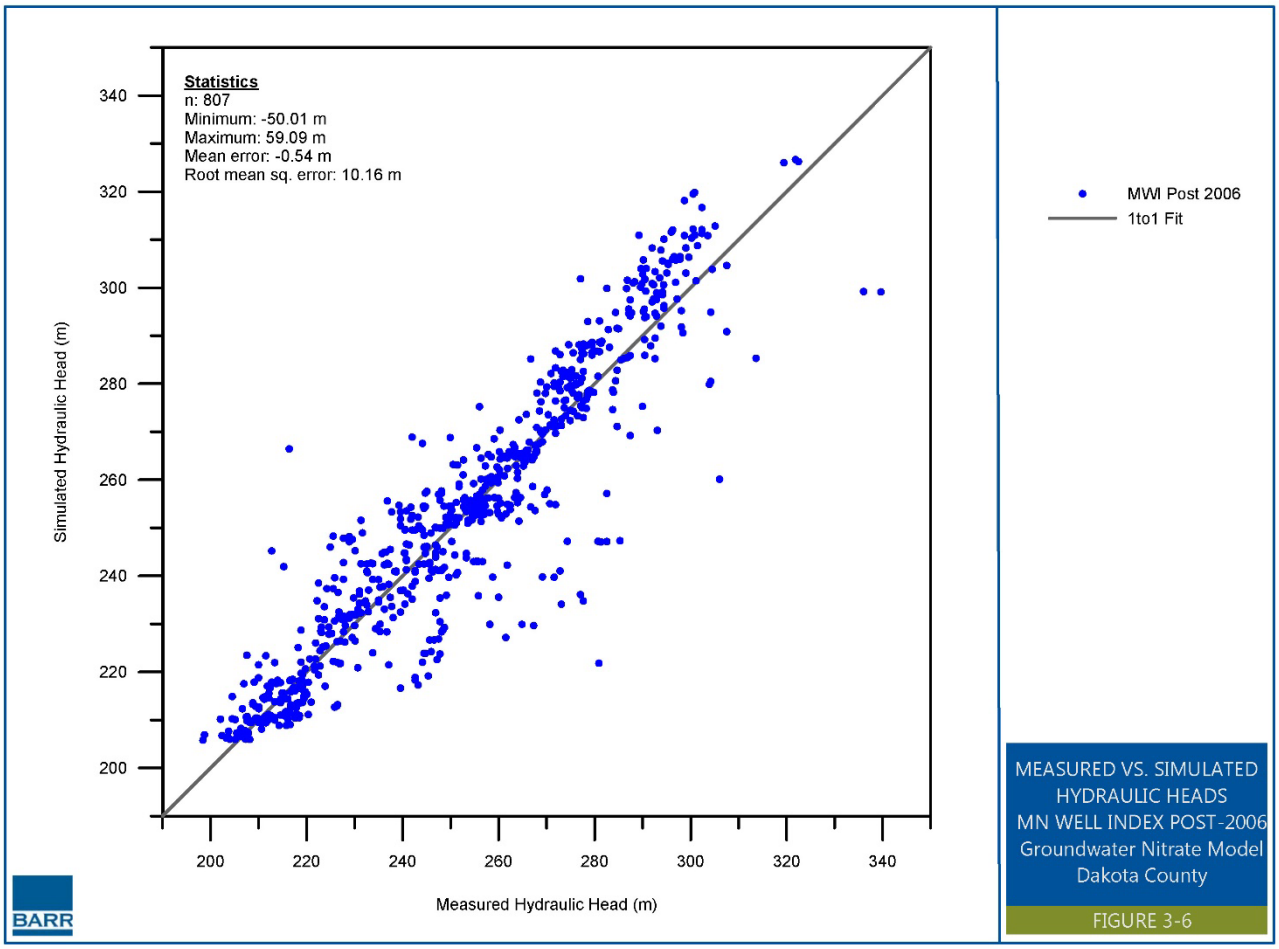

Figure 3-7 Measured vs Simulated Hydraulic Heads, Minnesota DNR Observations Wells

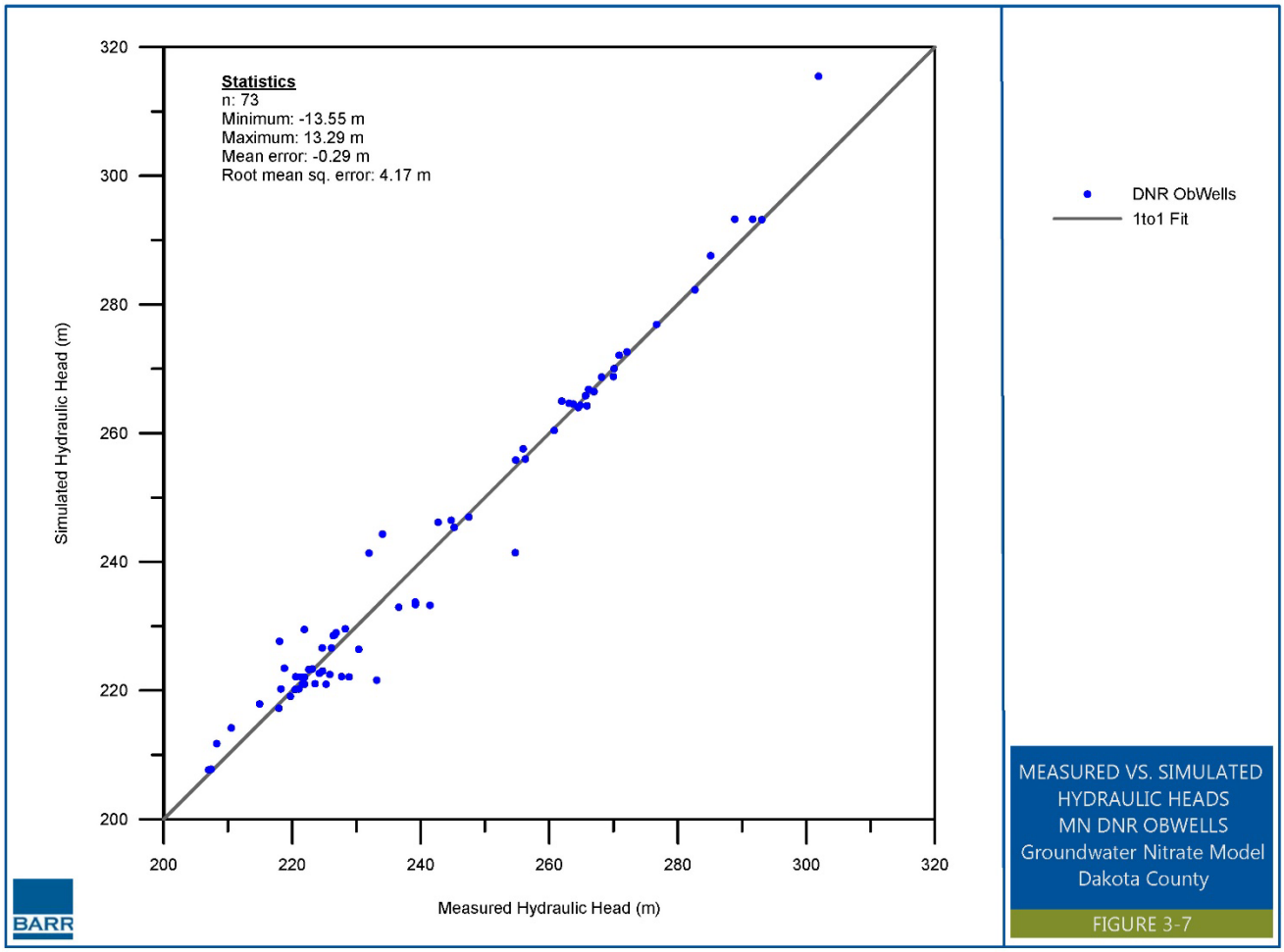

Figure 3-8 Measured vs Simulated Baseflow

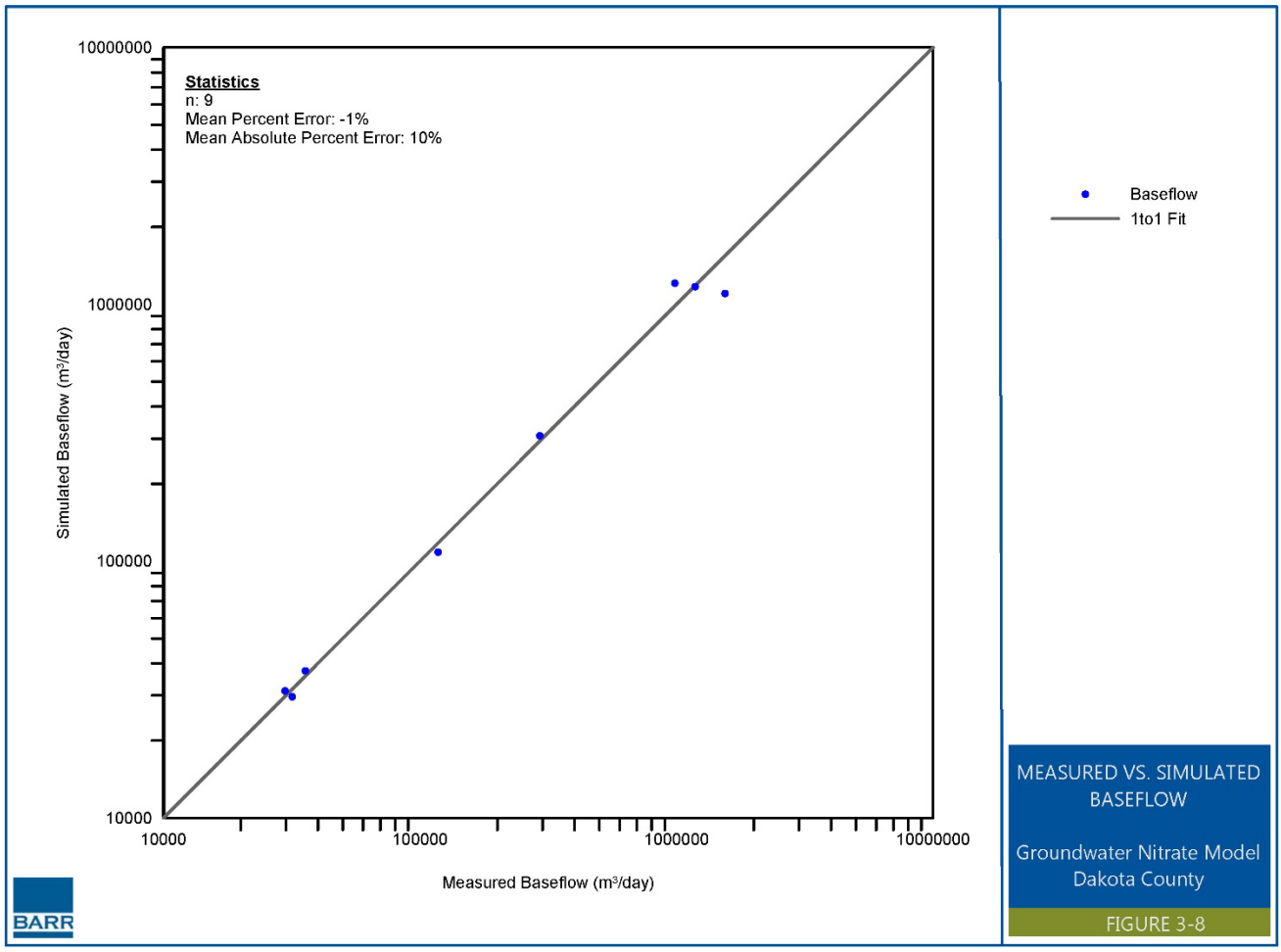

Figure 3-9 Measured vs Simulated Transmissivity

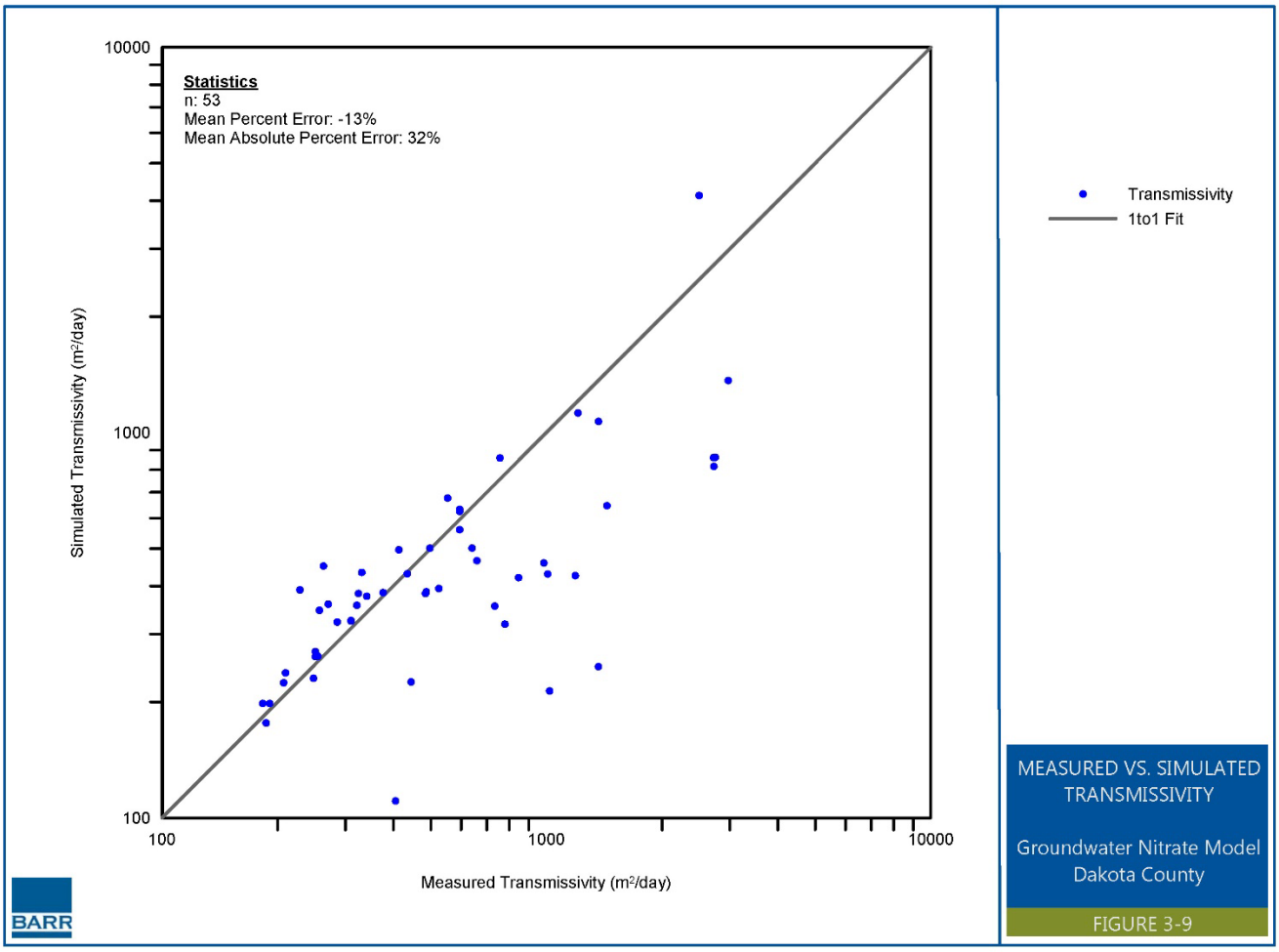

4 Simulation of Nitrate in Groundwater

To simulate nitrate in groundwater, the MODFLOW-based local groundwater flow model described in Section 3 was combined with the fate and transport model MT3D-USGS (Bedekar et.al., 2016). Nitrate leaching rates described in Section 2 were combined with the groundwater recharge of the MODFLOW model to obtain an infiltration concentration. The nitrate introduced to the groundwater flow system via infiltration was then tracked through the saturated zone to estimate the distribution of nitrate in groundwater across the County.

As described in Section 2, nitrate leaching was based on the MDA's modeling for areas of the Hastings DWSMA and mapped to the entire county using regressions based on the MDA modeling and soil organic carbon content percentage. Nitrate leaching for non-agricultural areas (developed areas) and pasture, alfalfa, and turf land covers were determined through a calibration procedure.

4.1 Calibration of Nitrate in Groundwater

As part of a calibration procedure, simulated nitrate concentrations were compared to measured nitrate concentrations from private wells provided by Dakota County. Due to the complexity of nitrate loading and transport, in addition to the scale of the study, calibration was focused on the township level. Data were tracked for individual wells but the goal of the model calibration process was to best capture nitrate trends in groundwater at the township level. Close inspection of the measured nitrate data shows areas where neighboring wells in the same aquifer have significantly different nitrate concentrations. At the scale of the model, it is not expected that the mechanisms that may drive these well-by-well differences are captured. Calibration was focused on the township level with a primary calibration target being the mean measured nitrate concentration for each township or municipality in Dakota County. For calibration purposes, the loading rate and groundwater flow field were both steady-state; pumping, recharge, and loading were simulated to represent constant averages. Simulated values after 50 years of transport in the groundwater flow system were used for comparison to measured values. Using simulated values beyond 50 years did not make any significant differences in the calibration. The measured values used for comparison to the simulated values are the most recent sampling data provided by Dakota County and represent a range in sampling dates between 2013 and 2020.

A limited number of parameters were adjusted during the nitrate calibration process. For leaching rates, the only adjustments that were made during calibration were for developed areas and for pasture, alfalfa and turf land covers; these areas were not simulated by MDA. Regressions described in Section 2 were used to map nitrate leaching to areas outside the MDA study area (Hastings DWSMA). The groundwater flow field, as determined by the groundwater flow model described in Section 3, was not adjusted as part of the nitrate calibration process. Additional model parameters that were adjusted during nitrate calibration include the porosity of unconsolidated and bedrock aquifers and a first-order decay rate that was used to represent potential denitrification processes.

4.2 Results of Nitrate in Groundwater Calibration and Baseline Loading

A plot of township-mean measured nitrate vs simulated nitrate at private wells is presented on Figure 4-1. Overall, general trends in nitrate concentration at the township scale are captured by the model. Figure 4-2 shows the simulated baseline nitrate concentration distribution across the County. The distribution of nitrate agrees favorably with interpolations of measured nitrate distributions. In general, nitrate concentrations in groundwater are greatest in the southeastern part of the County. Areas in the southwestern part of the County have less nitrate in groundwater even though loading rates are not significantly different from areas in the southeastern part of the County (Figure 4-3). The difference in the groundwater concentrations appears to be driven primarily by differences in geology. The southwestern part of County has lower permeability sediments (e.g. see Figure A-9 and A-10) which results in less recharge to the water table and lower flow velocities allowing for more denitrification along flow paths in these areas. The loading rates for the baseline simulation are presented on Figure 4-3.

The calibrated parameters associated with the nitrate calibration process are presented in Table 4-1 below.

Table 4-1 Nitrate in Groundwater Calibration Parameters

Parameter	Value
N loading for developed areas (non-agricultural areas)	15 lbs/acres
N loading for pasture, alfalfa, and turf	10 lbs/acre
1st order decay rate	1.0e-9 1/days
Porosity of Quaternary aquifer	0.2
Porosity of Decorah, Platteville, Glenwood aquifer	0.1
Porosity of St. Peter aquifer	0.25
Porosity of Prairie du Chien aquifer	0.08
Porosity of Jordan aquifer	0.22

Several scenarios were developed to evaluate changes in loading rates and how they may affect groundwater concentrations. These scenarios are and results presented in Section 5.

Figure 4-1 Measured vs Simulated Mean Nitrate-N per Township

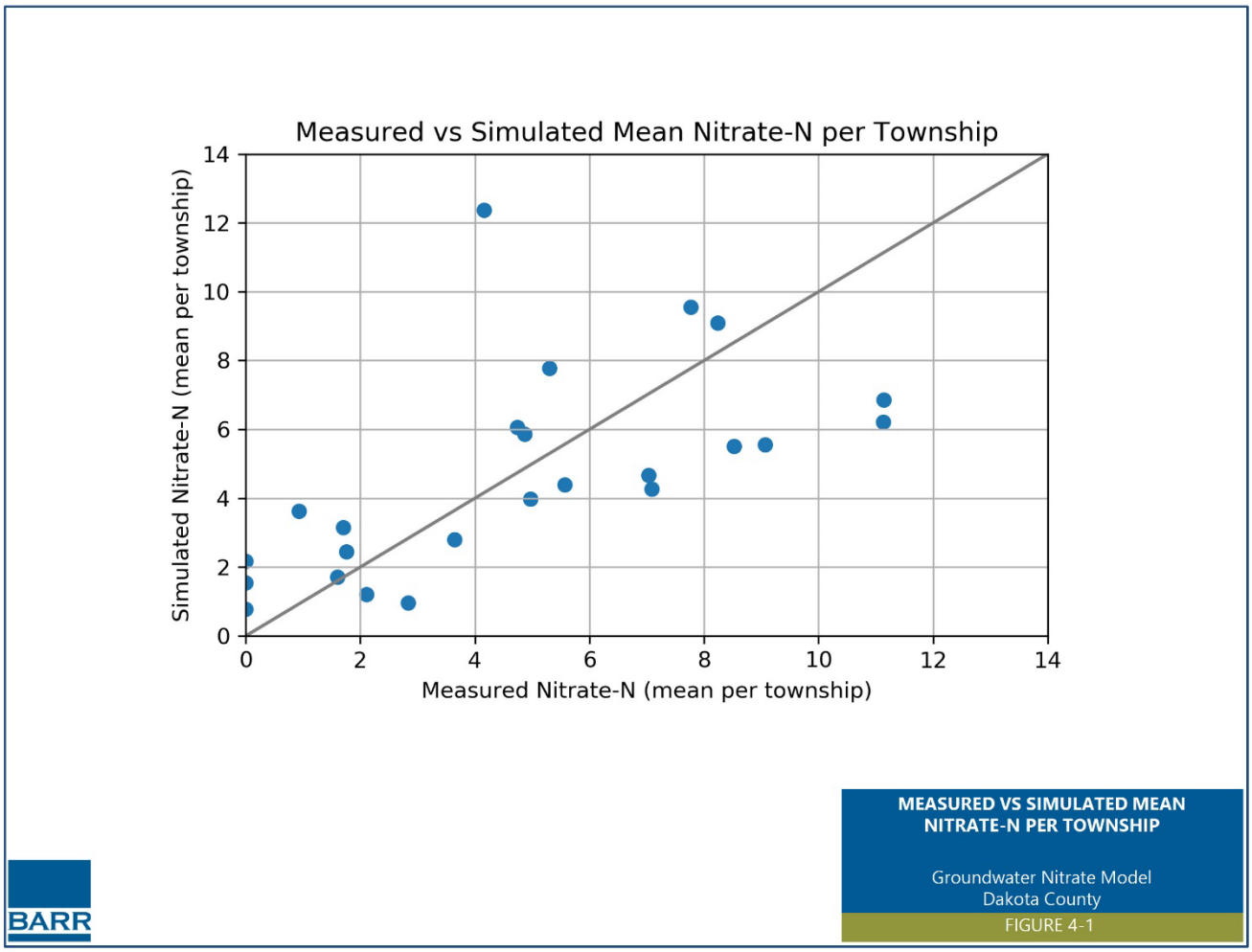

Figure 4-2 Baseline Simulated Nitrate-N

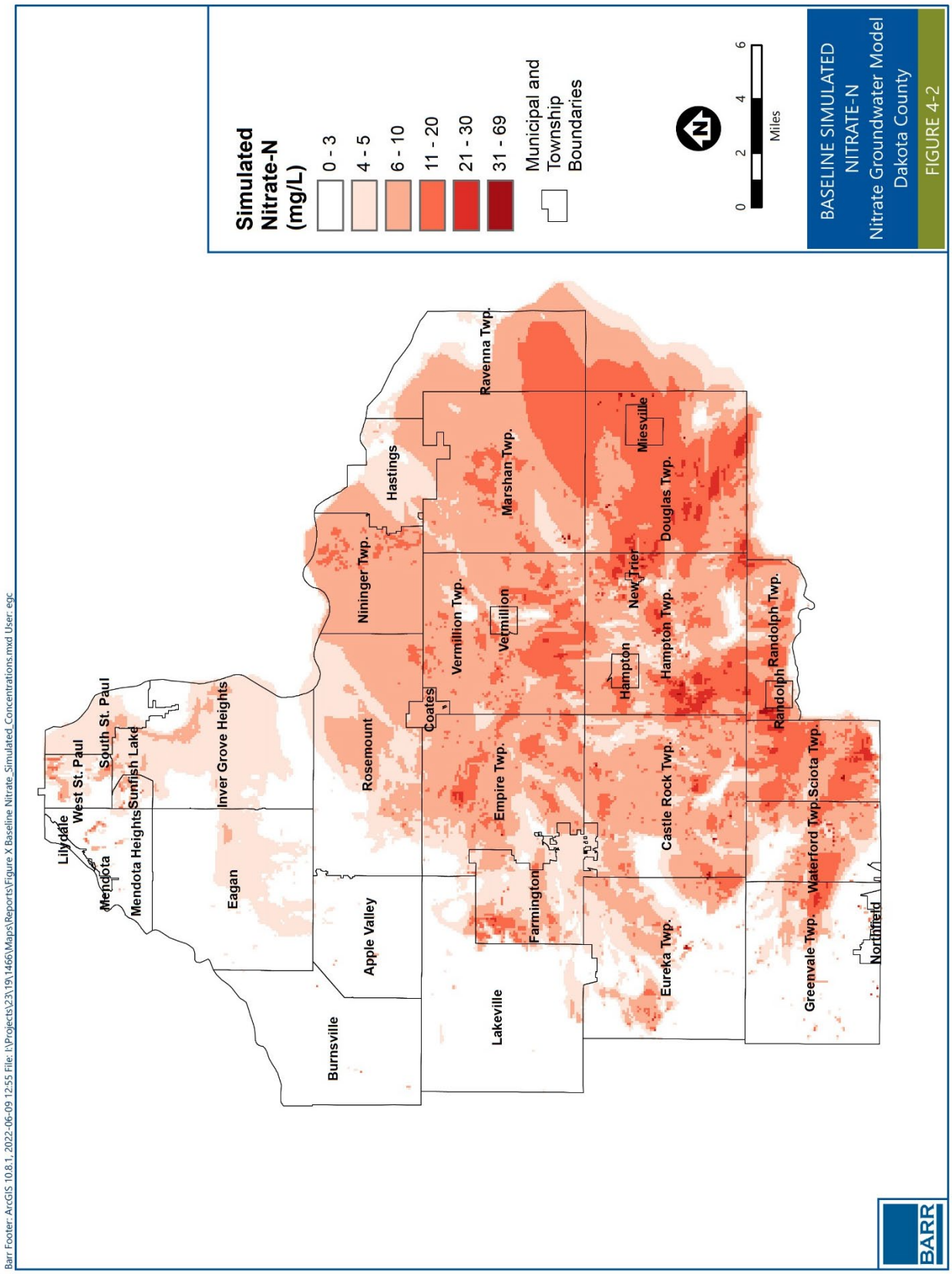

Figure 4-3 Simulated Nitrate-N Leaching Rate, Baseline

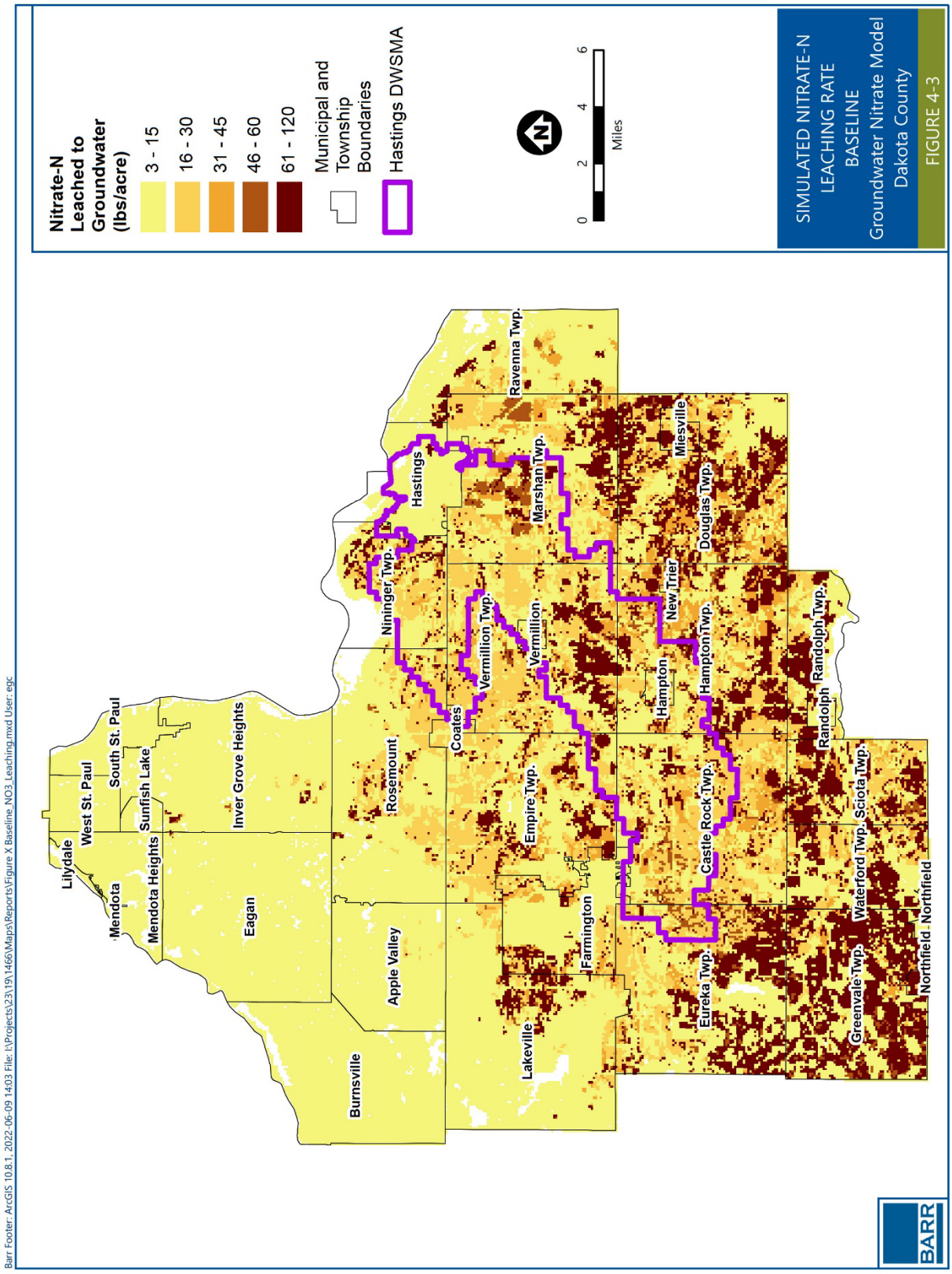

5 Modeling Scenarios

5.1 Nitrate Leaching Rate Reduction Estimates

As discussed in Section 2.1, MDA indicated that based on current cropland management within the Hastings DWSMA it is estimated that 3 and 4 percent of the respective irrigated and non-irrigated corn and soybean cropland is using cover crops. As a result, the average MDA nitrate leaching estimates for each scenario were weighted based on the relative cover crop areas for irrigated and non-irrigated corn and soybean cropland to simulate existing conditions. Following consultation with MDA, Dakota County recommended that three modeling scenarios should be simulated to evaluate the net effect on the weighted nitrate leaching rates, and associated changes in groundwater nitrate concentrations, from increased adoption of cover crops and/or conversion of cultivated cropland to perennials. Table 5-1 shows how the relative areas of cover crop adoption and perennial conversion for each of the three modeling scenarios compare to existing conditions, along with corresponding estimates of how the weighted average nitrate leaching rate from cropland will be reduced for each scenario.

Table 5-1 Irrigated and Non-Irrigated Agricultural Acreage by Crop Rotation

Scenario	Percent Non-Irrigated Cropland with Cover Crops	Percent Irrigated Cropland with Cover Crops	Percent Cropland as Perennials	Estimated Reduction in Weighted Nitrate Leaching Rate from Cropland
Existing Conditions (Baseline)	4%	3%	0%	--
Scenario 1	20%	20%	5%	6%
Scenario 2	40%	40%	5%	13%
Scenario 3	20%	20%	8%	14%

For each scenario nitrate leaching rates simulated in the model were updated to reflect the changes outlined in Table 5-1. The model was then run and results summarized on a township level. Figure 5-1 to Figure 5-4 present the median concentration of Nitrate-N in each township or municipality. These results are also summarized in Table 5-2.

Table 5-2 Median groundwater nitrate concentrations in mg/L for each scenario

Name	Baseline	Scenario 1	Scenario 1 % Change from Baseline	Scenario 2	Scenario 2 % Change from Baseline	Scenario 3	Scenario 3 % Change from Baseline
Apple Valley	1.7	1.7	0%	1.7	0%	1.7	0%
Burnsville	1.0	1.0	0%	1.0	0%	1.0	0%
Castle Rock Twp.	6.6	6.3	-5%	5.9	-11%	5.8	-12%
Coates	6.4	6.1	-5%	5.7	-11%	5.6	-12%
Douglas Twp.	11.9	11.2	-6%	10.5	-12%	10.4	-13%
Eagan	2.7	2.7	0%	2.7	0%	2.7	0%
Empire Twp.	6.4	6.1	-5%	5.7	-10%	5.7	-11%
Eureka Twp.	2.6	2.5	-4%	2.4	-9%	2.3	-9%
Farmington	4.6	4.5	-3%	4.3	-7%	4.3	-8%
Greenvale Twp.	1.1	1.0	-5%	1.0	-11%	1.0	-12%
Hampton	6.7	6.4	-4%	6.1	-9%	6.0	-10%
Hampton Twp.	7.8	7.4	-5%	6.9	-11%	6.8	-12%
Hastings	4.6	4.4	-3%	4.3	-7%	4.2	-8%
Inver Grove Heights	3.6	3.5	-1%	3.5	-2%	3.5	-2%
Lakeville	0.6	0.6	-1%	0.6	-2%	0.6	-2%
Marshan Twp.	7.2	6.8	-5%	6.3	-11%	6.3	-12%
Mendota	0.1	0.1	0%	0.1	0%	0.1	0%
Mendota Heights	1.0	1.0	0%	1.0	0%	1.0	0%
Miesville	14.3	13.5	-6%	12.5	-13%	12.3	-14%
New Trier	11.0	10.3	-6%	9.7	-12%	9.6	-13%
Nininger Twp.	7.1	6.7	-5%	6.3	-11%	6.3	-12%
Northfield	0.3	0.3	-6%	0.3	-12%	0.3	-13%
Randolph	9.3	8.9	-5%	8.4	-10%	8.3	-11%
Randolph Twp.	8.3	7.9	-5%	7.4	-11%	7.3	-12%
Ravenna Twp.	6.1	5.8	-5%	5.4	-11%	5.4	-12%
Rosemount	4.7	4.6	-4%	4.4	-7%	4.3	-8%
Sciota Twp.	10.3	9.8	-6%	9.1	-12%	9.0	-13%
South St. Paul	3.9	3.9	0%	3.9	0%	3.9	0%
Sunfish Lake	3.4	3.4	0%	3.3	-1%	3.3	-1%
Vermillion	5.2	5.0	-5%	4.6	-12%	4.6	-13%
Vermillion Twp.	7.7	7.3	-5%	6.8	-12%	6.7	-13%
Waterford Twp.	5.6	5.3	-5%	5.0	-11%	4.9	-12%

Figure 5-1 Median Simulated Nitrate-N, Baseline Scenario

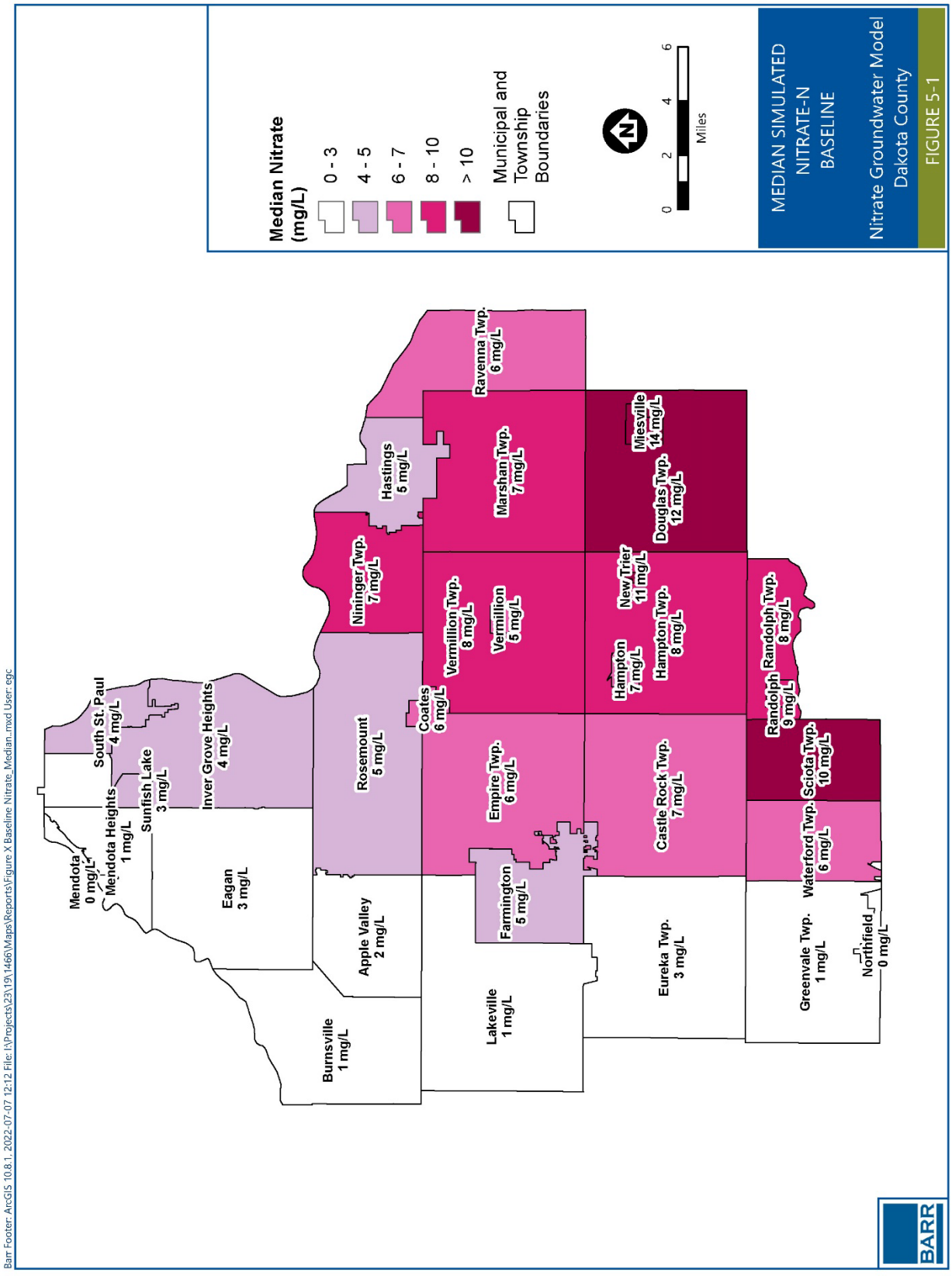

Figure 5-2 Median Simulated Nitrate-N, Scenario 1

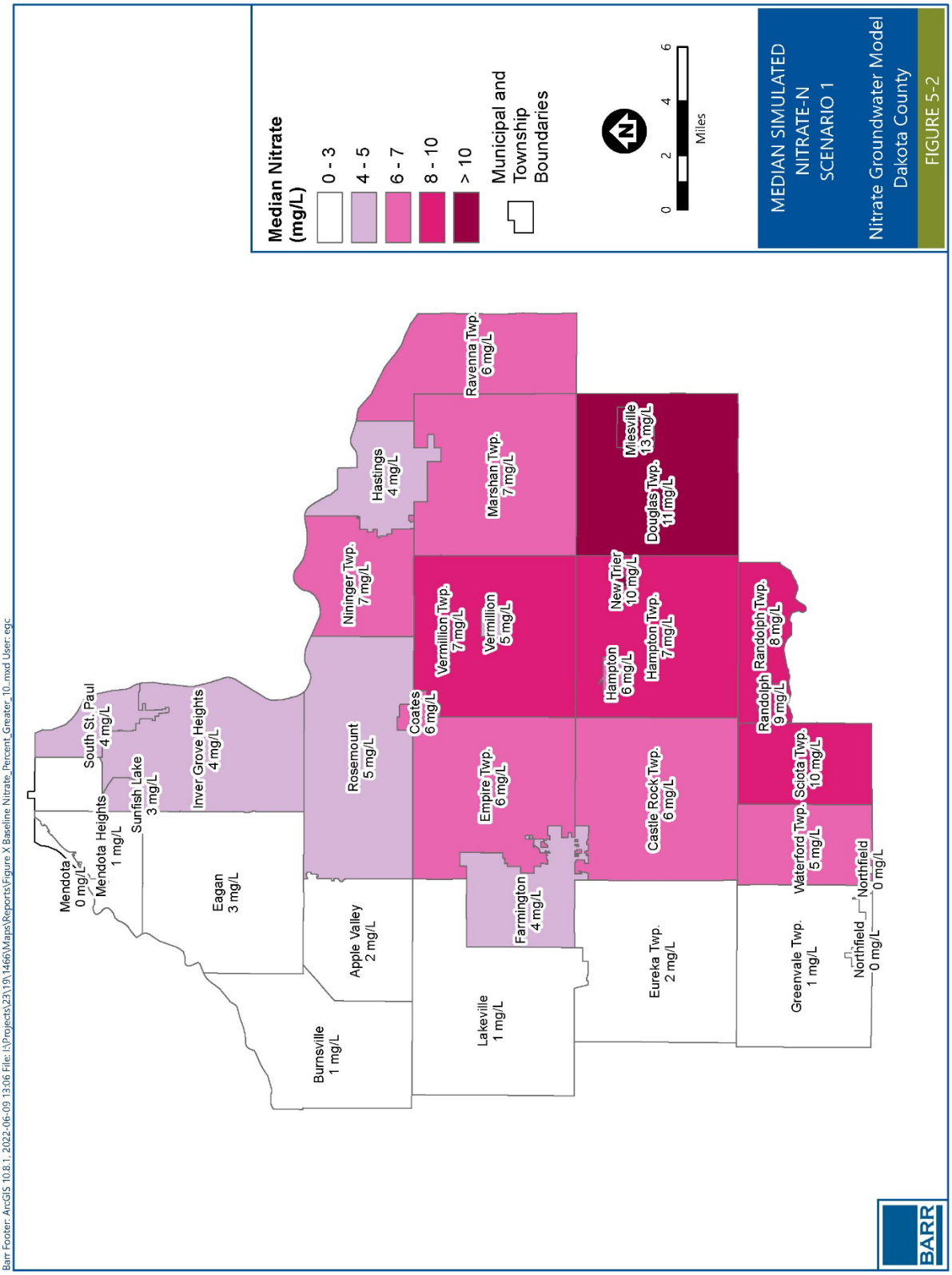

Figure 5-3 Median Simulated Nitrate-N, Scenario 2

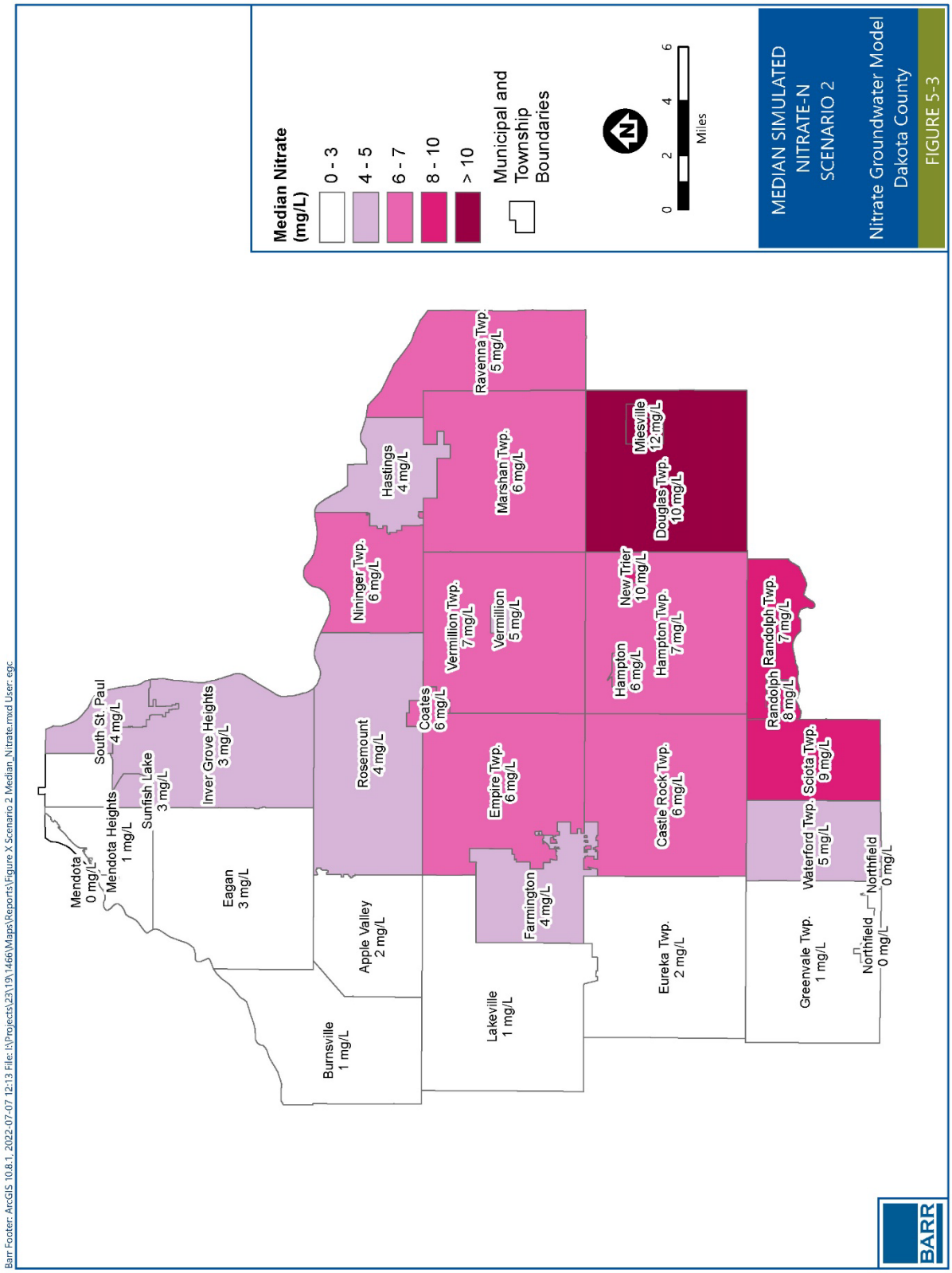

Figure 5-4 Median Simulated Nitrate-N, Scenario 3

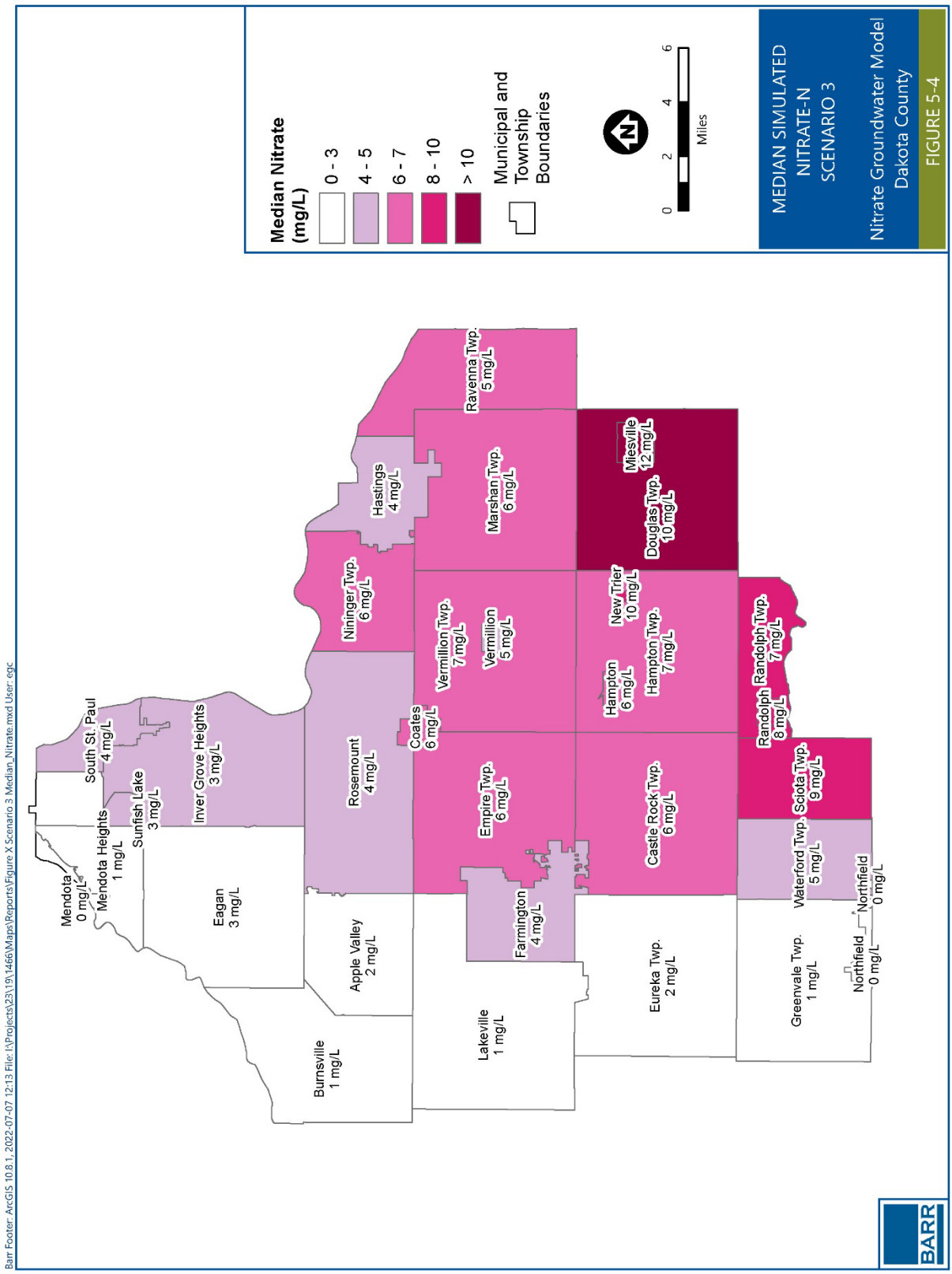

6 Summary and Recommendations

A local-scale MODFLOW groundwater flow model derived from Metro Model 3 was combined with the fate and transport model MT3D-USGS to simulate nitrate concentrations in groundwater in Dakota County. Leaching loss rates for current crop practices were obtained from the MDA for the Hastings DWSMA. This information was then reviewed and analyzed to map nitrate leaching rates to areas of the County outside of the Hastings DWSMA. The model reasonably simulates current nitrate concentrations in groundwater at a township level but the model is too large of a scale to accurately simulate nitrate at the individual well level.

Three modeling scenarios were simulated to evaluate the net effect on the weighted nitrate leaching rates, and associated changes in groundwater nitrate concentrations, from increased adoption of cover crops and/or conversion of cultivated cropland to perennials. These scenarios were summarized based on the median nitrate-N for shallow groundwater within each township or municipality and compared to the baseline (existing conditions) simulation. The scenarios show a reduction in the median nitrate-N for each township.

The modeling results presented in this report illustrate that reductions of nitrate-N in groundwater may be achieved with increased adoption of cover crops and/or conversion of cultivated cropland to perennials. Implementing the following recommendations would be expected to provide information to improve the groundwater model and simulation of the different scenarios.

- Simulate leaching rates for areas outside of the Hastings DWSMA. Soil leaching rates were developed by MDA for areas of the Hastings DWSMA. For this study, these leaching rates were mapped to other areas of the county based on soil organic carbon content.
- Collect site specific groundwater quality data at the scale of individual fields to compare the water quality data to modeled nitrate concentrations. Results of the comparisons can then be used to assess the appropriateness of the leaching rates estimated by the MDA modeling.
- Work with producers to determine if application rates assumed for the MDA study reflect actual application rates.
- Monitor groundwater quality through time at established locations to track temporal changes. Compare these changes to predicted changes from the modeling. Reevaluate or recalibrate the model as needed based on these new data.
- Establish long term stream nitrate monitoring to capture watershed scale changes. During baseflow conditions these data may represent larger scale groundwater quality and help to integrate what is seen at individual wells. To make these data most useful, discharge should also be measured at the time of sampling.

7 References

Anderson, M.P. and W.W. Woessner, 1992. Applied Groundwater Modeling, Simulation of Flow and Advective Transport. Academic Press, Inc., New York, New York, 381 p

Barr Engineering, 2010. Evaluation of groundwater and surface-water interaction: guidance for resources assessment, Twin Cities metropolitan area, Minnesota. Prepared for Metropolitan Council, June 2010. 27p. plus GIS files.

Bedekar, V., Morway, E.D., Langevin, C.D., and Tonkin, M., 2016, MT3D-USGS version 1: A U.S. Geological Survey release of MT3DMS updated with new and expanded transport capabilities for use with MODFLOW: U.S. Geological Survey Techniques and Methods 6-A53, 69 p., http://dx.doi.org/10.3133/tm6A53

Doherty, J., 2013, Addendum to the PEST manual: Brisbane, Australia, Watermark Numerical Computing

Doherty, J., 2010a, PEST, Model-independent parameter estimation—User manual, 5th ed.: Brisbane, Australia, Watermark Numerical Computing

Doherty, J., 2010b, Windows BEOPEST. Watermark Numerical Computing

Doherty, J., 2003, Groundwater model calibration using pilot-points and regularization: Ground Water, v. 41, no. 2, p. 170–177

Doherty, J.E., Fienen, M.N., and Hunt, R.J., 2010, Approaches to highly parameterized inversion: Pilot-point theory, guidelines, and research directions: U.S. Geological Survey Scientific Investigations Report 2010–5168, 36 p

Dripps W.R. and K.R. Bradbury. 2007. A simple daily soil-water balance model for estimating the spatial and temporal distribution of groundwater recharge in temperate humid areas. Hydrogeology Journal 15, 433-444

Fienen, M.N., Muffels, C.T., and Hunt, R.J., 2009, On constraining pilot point calibration with regularization in PEST: Ground Water, v. 47, no. 6, p. 835–844.

Fienen, M.N., 2005. The three-point problem, vector analysis and extension to the n-point problem. Journal of Geoscience Education, v. 53, n. 3, p. 257-262.

Freeze, R.A. and J.A. Cherry, 1979. *Groundwater*. Prentice Hall, Upper Saddle River, NJ.

Hanson, R.T., Boyce, S.E., Schmid, Wolfgang, Hughes, J.D., Mehl, S.M., Leake, S.A., Maddock, Thomas, III, and Niswonger, R.G., 2014. One-Water Hydrologic Flow Model (MODFLOW-OWHM). U.S. Geological Survey Techniques and Methods 6-A51, 120 p.

Hill, M.C. and C.R. Tiedman. 2007. Effective groundwater model calibration: with analysis of data, sensitivities, predictions, and uncertainty, New Jersey, John Wiley & Sones, Inc., 455p.

Hobbs, H.C. and J.E., Goebel, 1982. Geologic map of Minnesota, Quaternary geology: Minnesota Geological Survey, State Map Series S-01, scale 1:500,000.

Mehl, S.W., and Hill, M.C., 2013, MODFLOW–LGR—Documentation of ghost node local grid refinement (LGR2) for multiple areas and the boundary flow and head (BFH2) package: U.S. Geological Survey Techniques and Methods book 6, chap. A44, 43 p

Metropolitan Council, 2016. *Regional Water Supply, Groundwater Recharge and Stormwater Reuse Study (Southeast Metro Study Area)*. Prepared by HDR Engineering, Inc. Metropolitan Council: Saint Paul.

Metropolitan Council, 2014. Twin Cities Metropolitan Area Regional Groundwater Flow Model, Version 3.0. Prepared by Barr Engineering. Metropolitan Council: Saint Paul, MN.

Metropolitan Council, 2012a. Using the soil water balance model (SWB) to estimate recharge for the Twin Cities Metropolitan Area Groundwater Model Version 3. Prepared by Barr Engineering. Metropolitan Council: Saint Paul, MN.

Metropolitan Council, 2012b. Groundwater contamination plumes. Unpublished data.

Mossler, J.H., 2013. Bedrock geology of the Twin Cities ten-county metropolitan area, Minnesota. Miscellaneous Map Series M-194, Minnesota Geological Survey.

Niswonger, R.G., Panday, S., and Ibaraki, M., 2011. MODFLOW-NWT, A Newton formulation for MODFLOW-2005. U.S. Geological Survey Techniques and Methods 6-A37, 44 p.

Runkel, A.C., Tipping, R.G., Alexander, E.C. Jr., Green, J.A., Mossler, J.H., and Alexander, S.C.. 2003. Hydrogeology of the Paleozoic Bedrock in Southeastern Minnesota. Minnesota Geological Survey Report of Investigations 61.

Spitz, K. and Moreno, J. 1996. A practical guide to groundwater flow and solute transport modeling: New York, John Wiley and Sons, 426p.)

Tikhonov, A.N., 1963a, Solution of incorrectly formulated problems and the regularization method: Soviet Math. Dokl., v. 4, p. 1035–1038.

Tipping, R.G. 2011. Distribution of vertical recharge to upper bedrock aquifers, Twin Cities metropolitan area. Minnesota Geological Survey report submitted to Metropolitan Council, November, 2011.l

Appendix A

Hydraulic Conductivity and Infiltration Distribution

Dakota County Groundwater Nitrate Model

Figure A-1 Horizontal Hydraulic Conductivity: Decorah-Platteville-Glenwood Formation

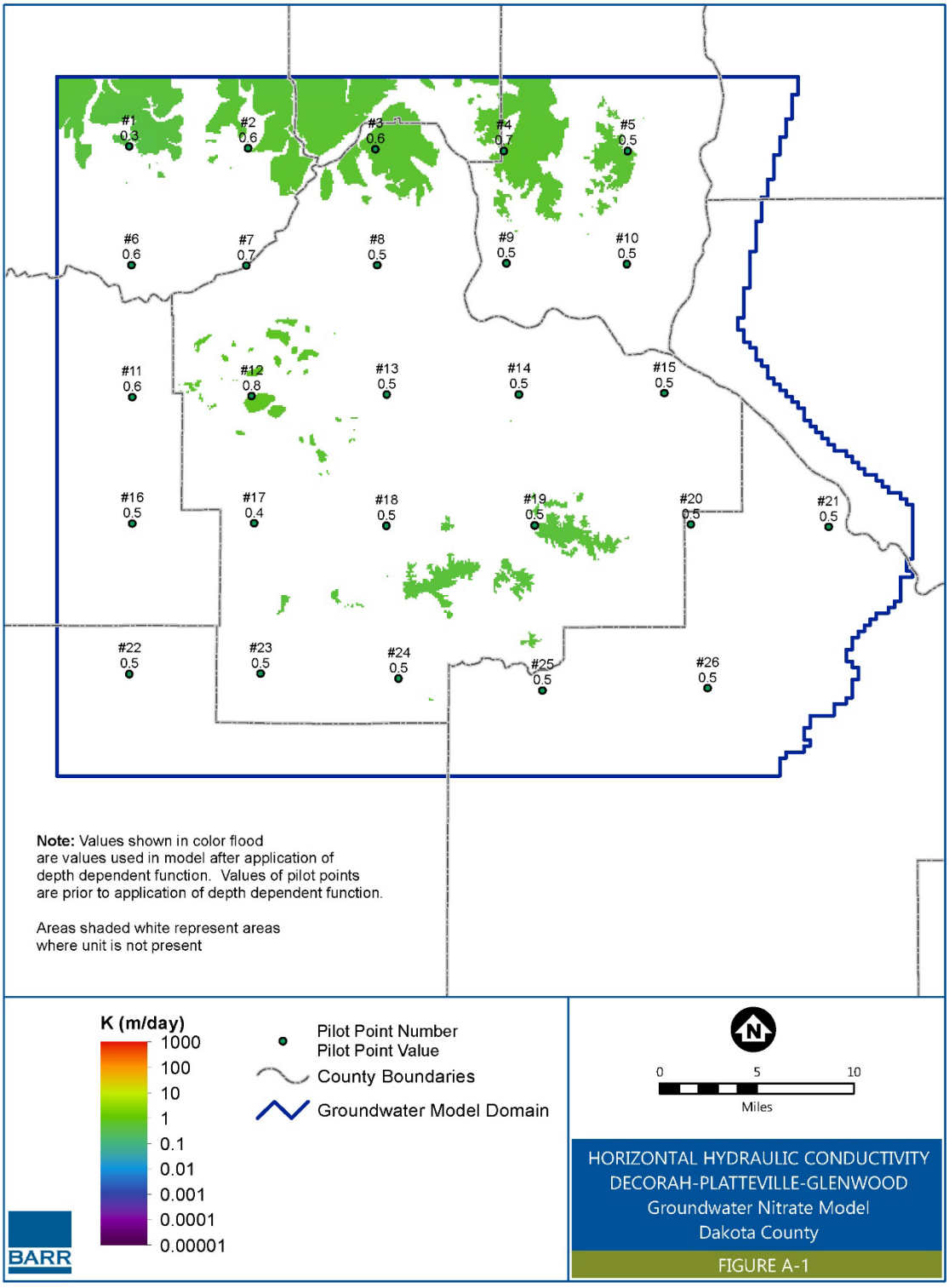

Figure A-2 Vertical Hydraulic Conductivity: Decorah-Platteville-Glenwood Formation

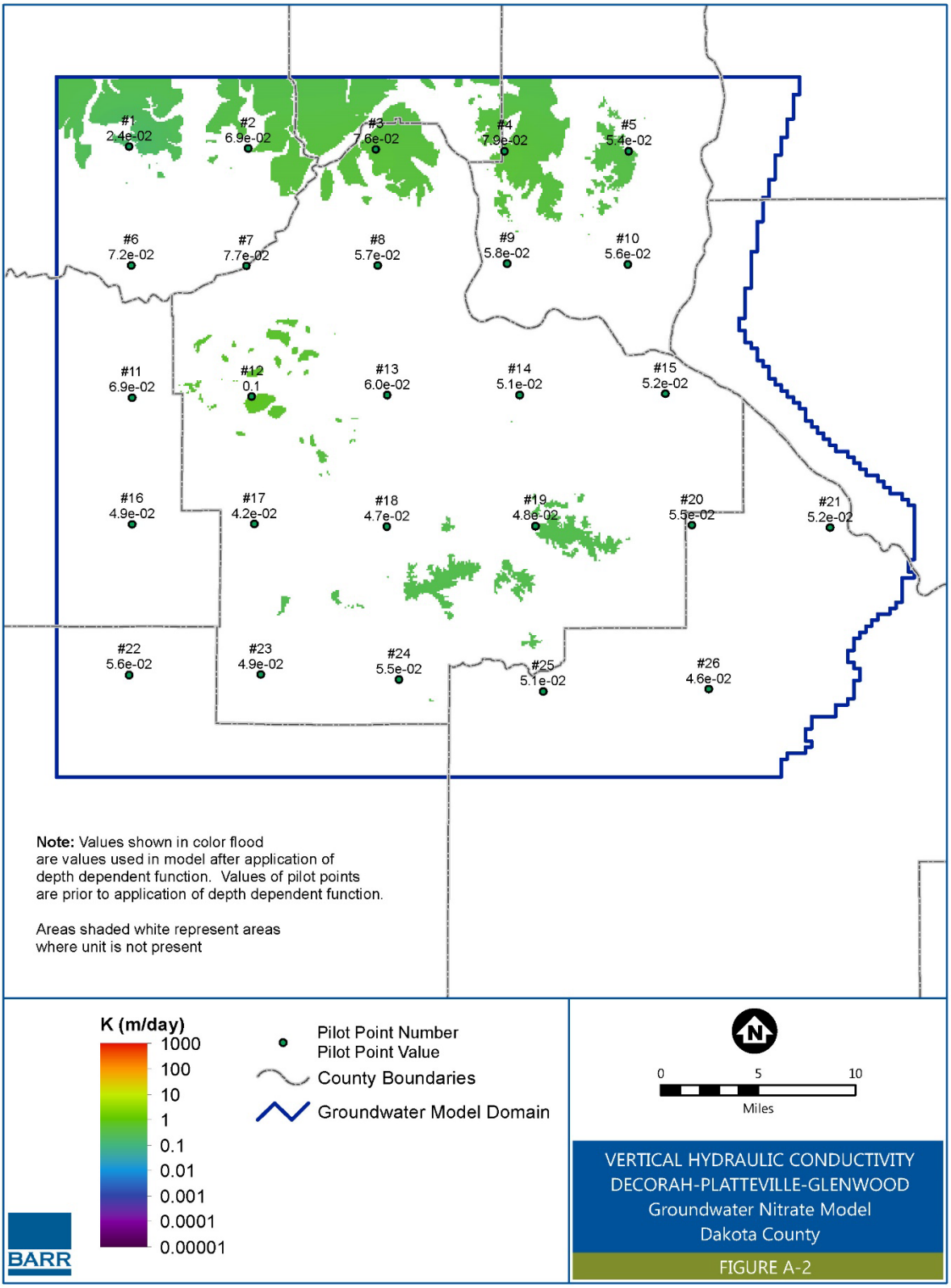

Figure A-3 Horizontal Hydraulic Conductivity: St. Peter Sandstone Formation

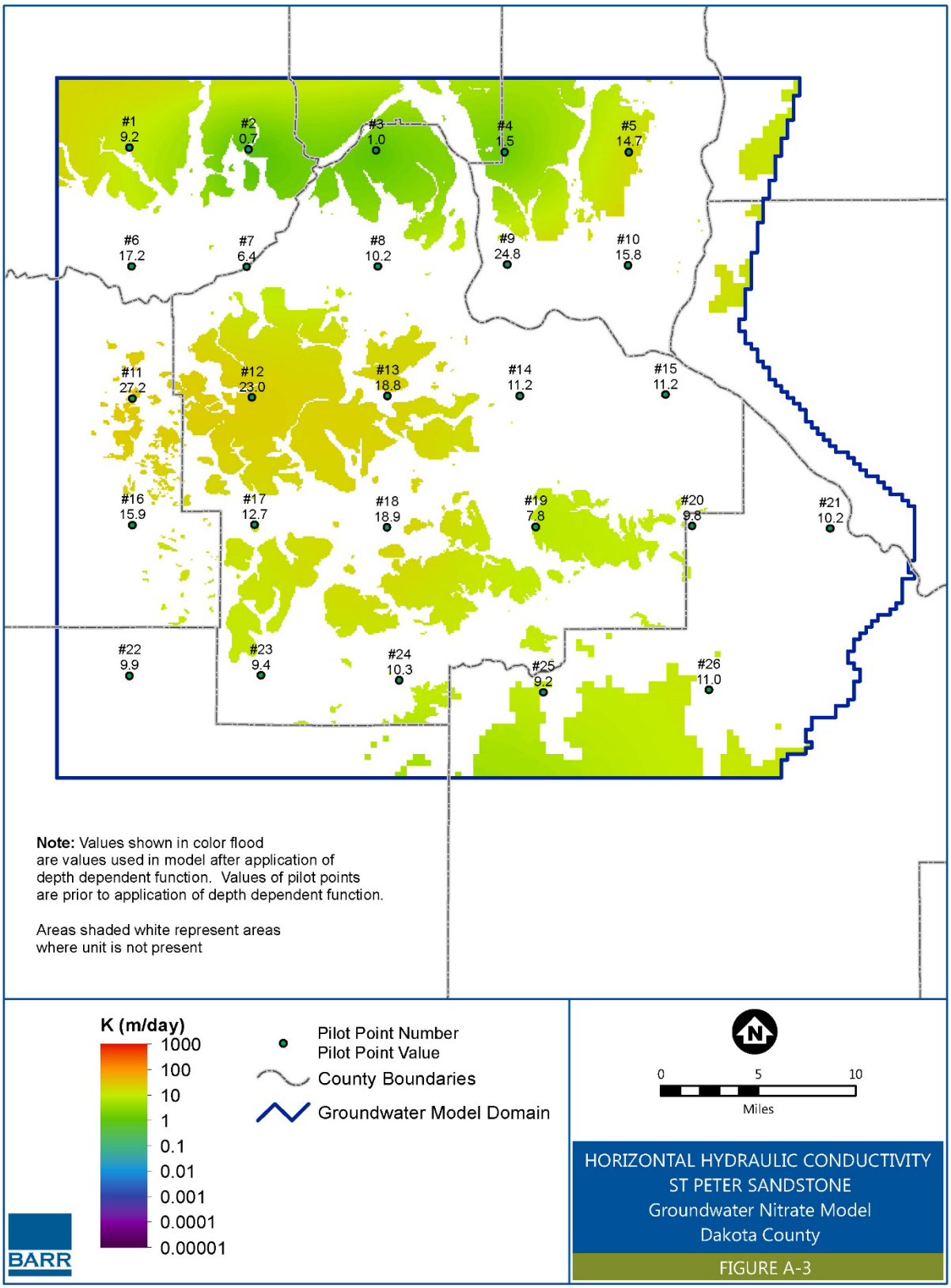

Figure A-4 Vertical Hydraulic Conductivity: St. Peter Sandstone Formation

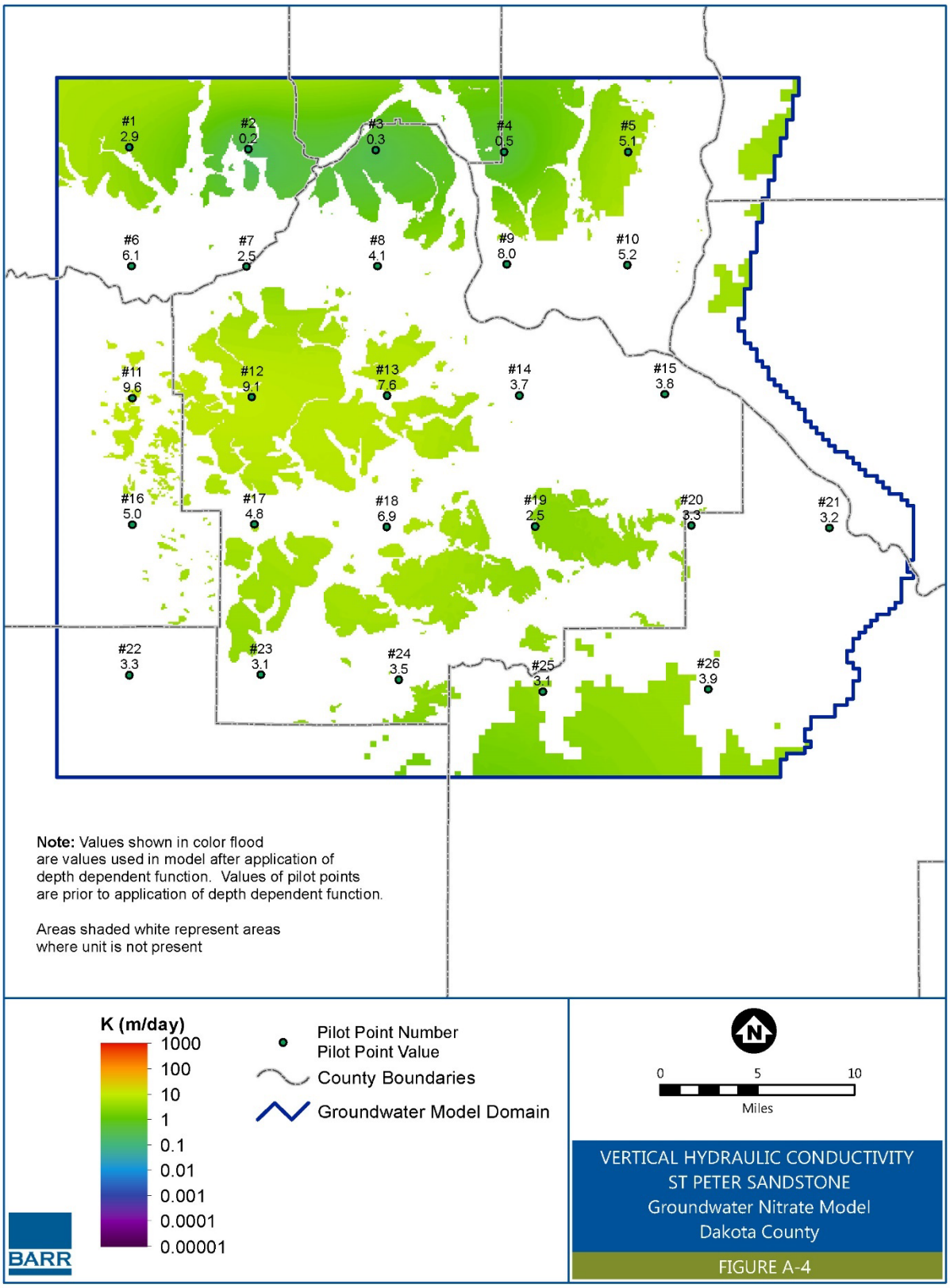

Figure A-5 Horizontal Hydraulic Conductivity: Prairie du Chien Group Formation

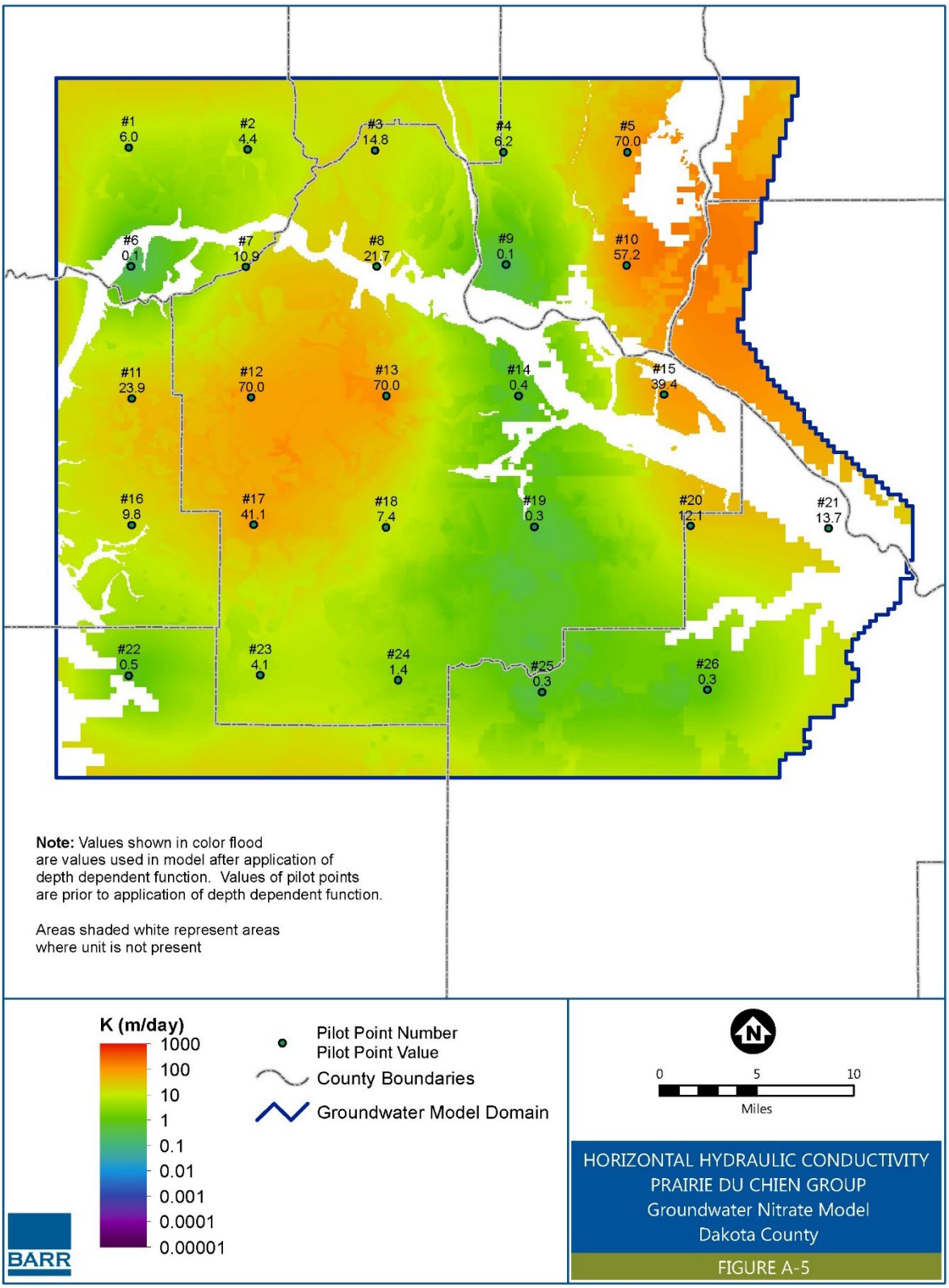

Figure A-6 Vertical Hydraulic Conductivity: Prairie du Chien Group Formation

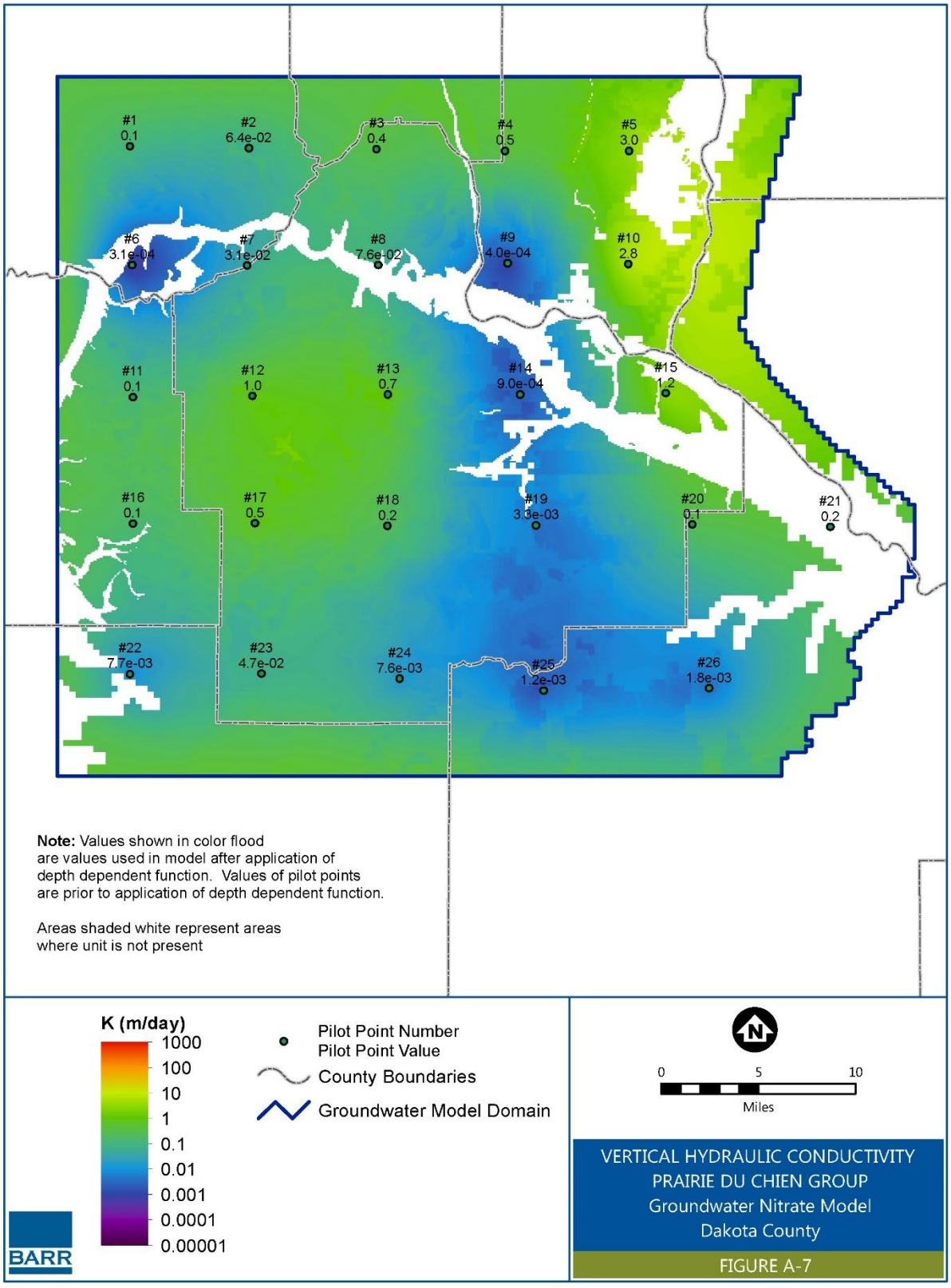

Figure A-7 Horizontal Hydraulic Conductivity: Jordan Sandstone Formation

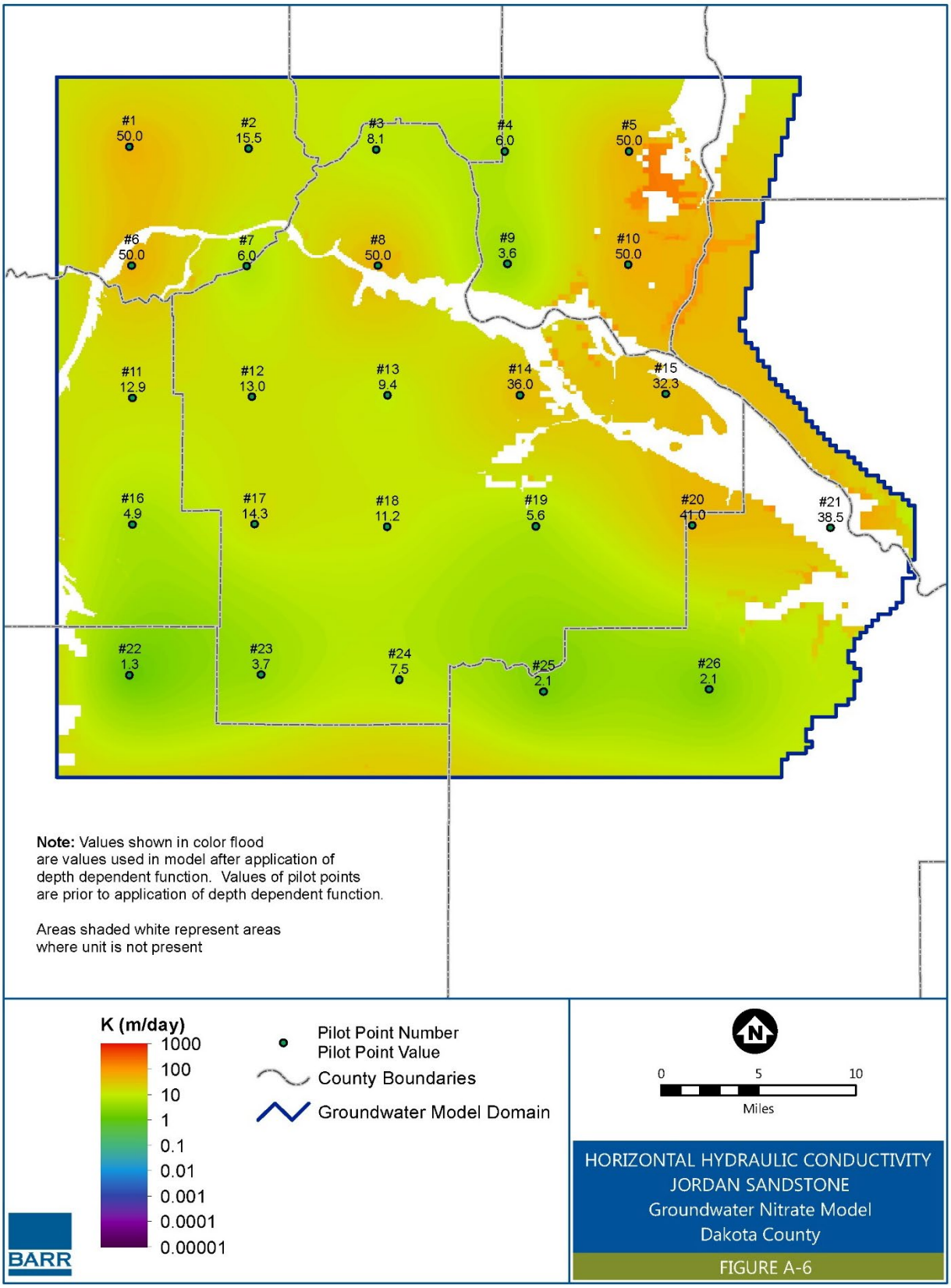

Figure A-8 Vertical Hydraulic Conductivity: Jordan Sandstone Formation

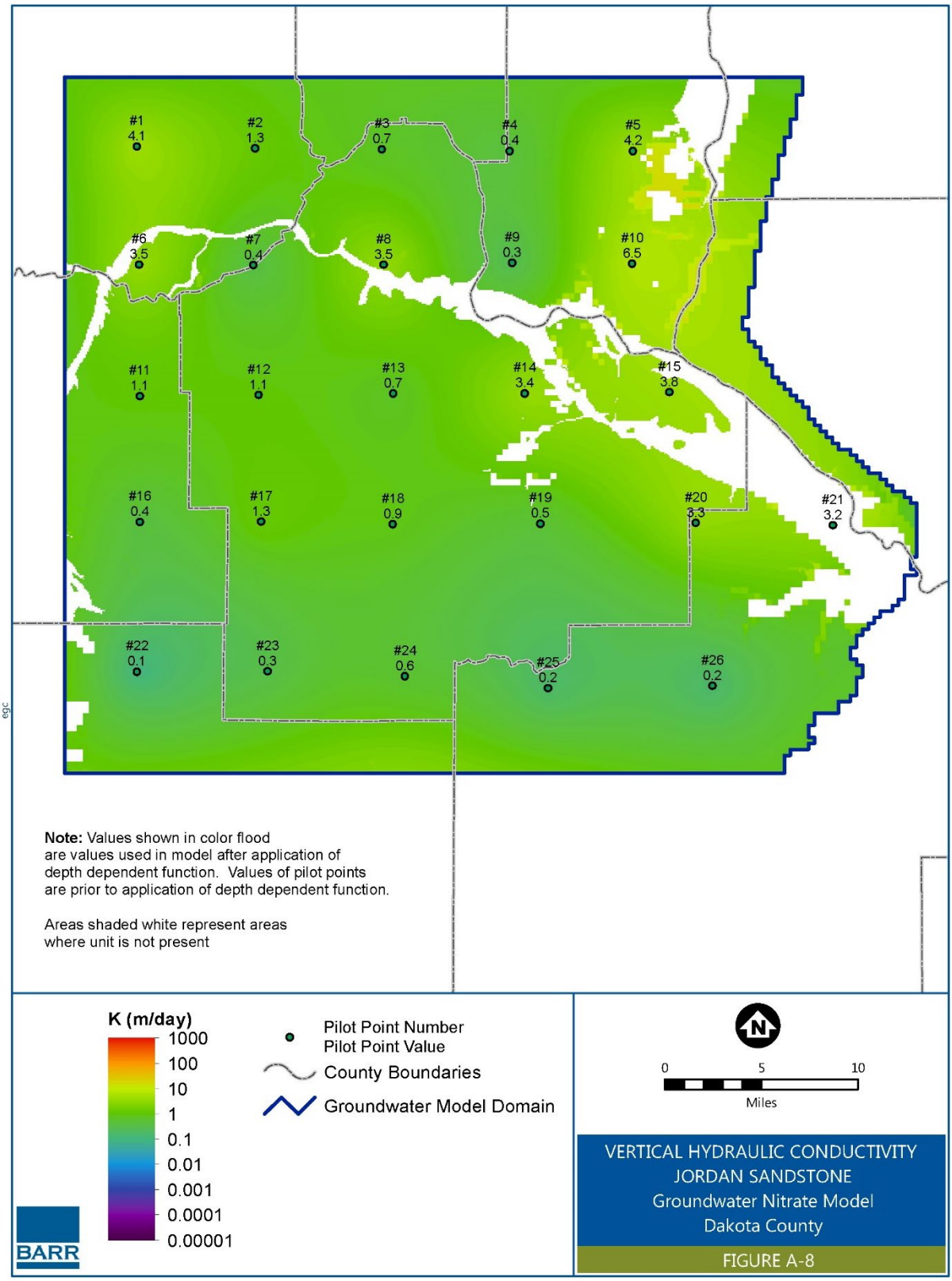

Figure A-9 Horizontal Hydraulic Conductivity: Quaternary Sediments Layer 1

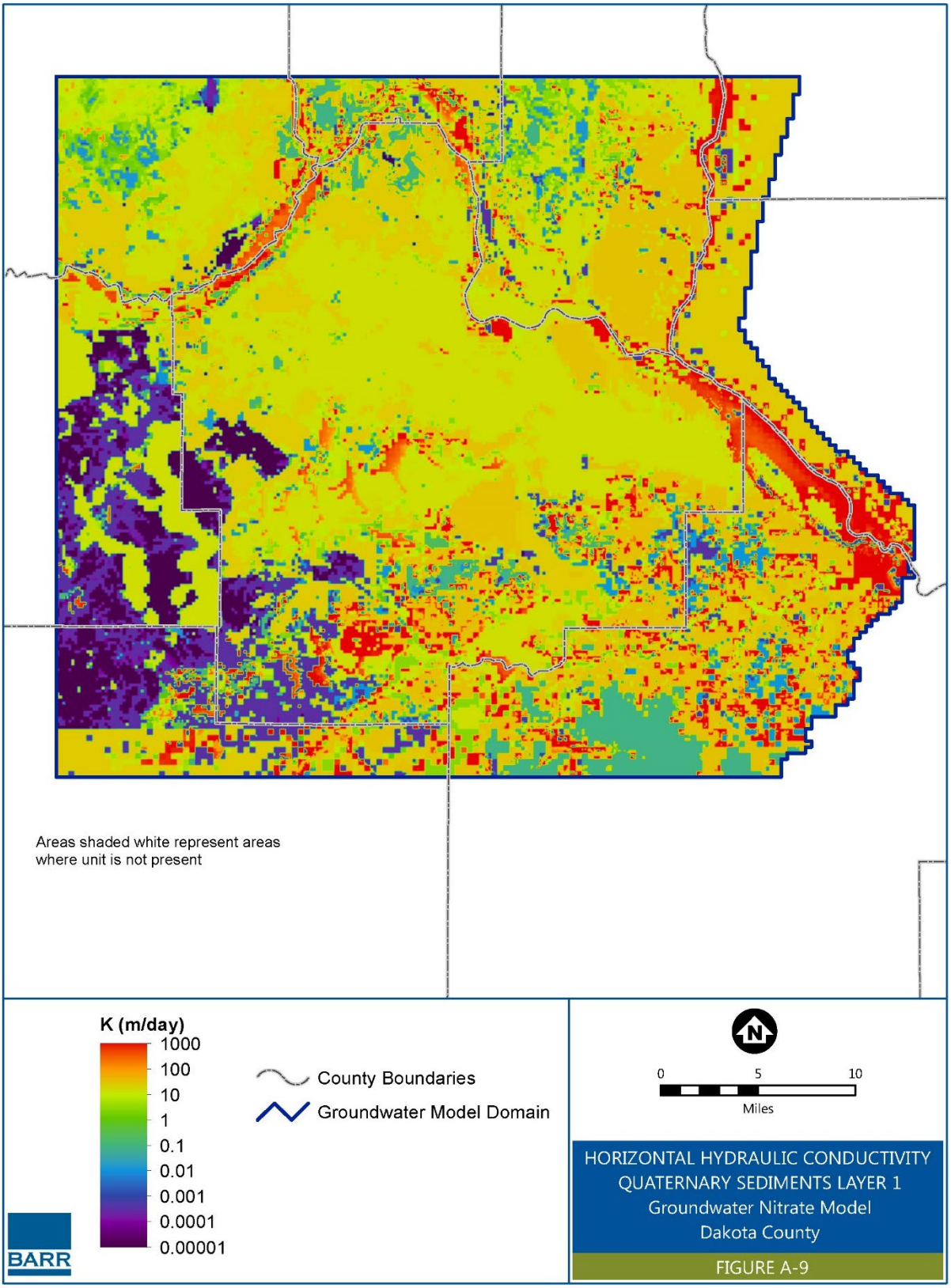

Figure A-10 Vertical Hydraulic Conductivity: Quaternary Sediments Layer 1

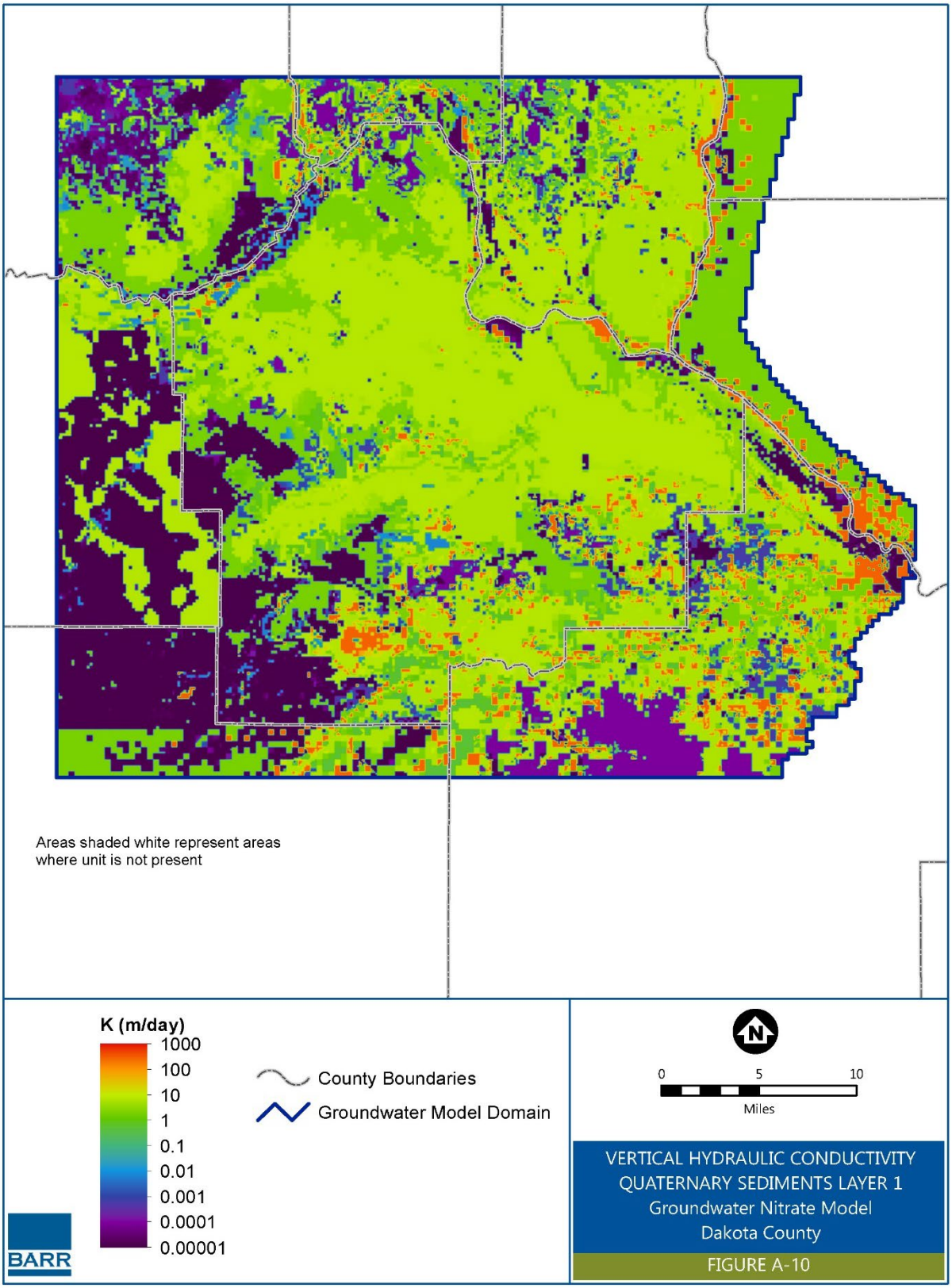

Figure A-11 Horizontal Hydraulic Conductivity: Quaternary Sediments Layer 2

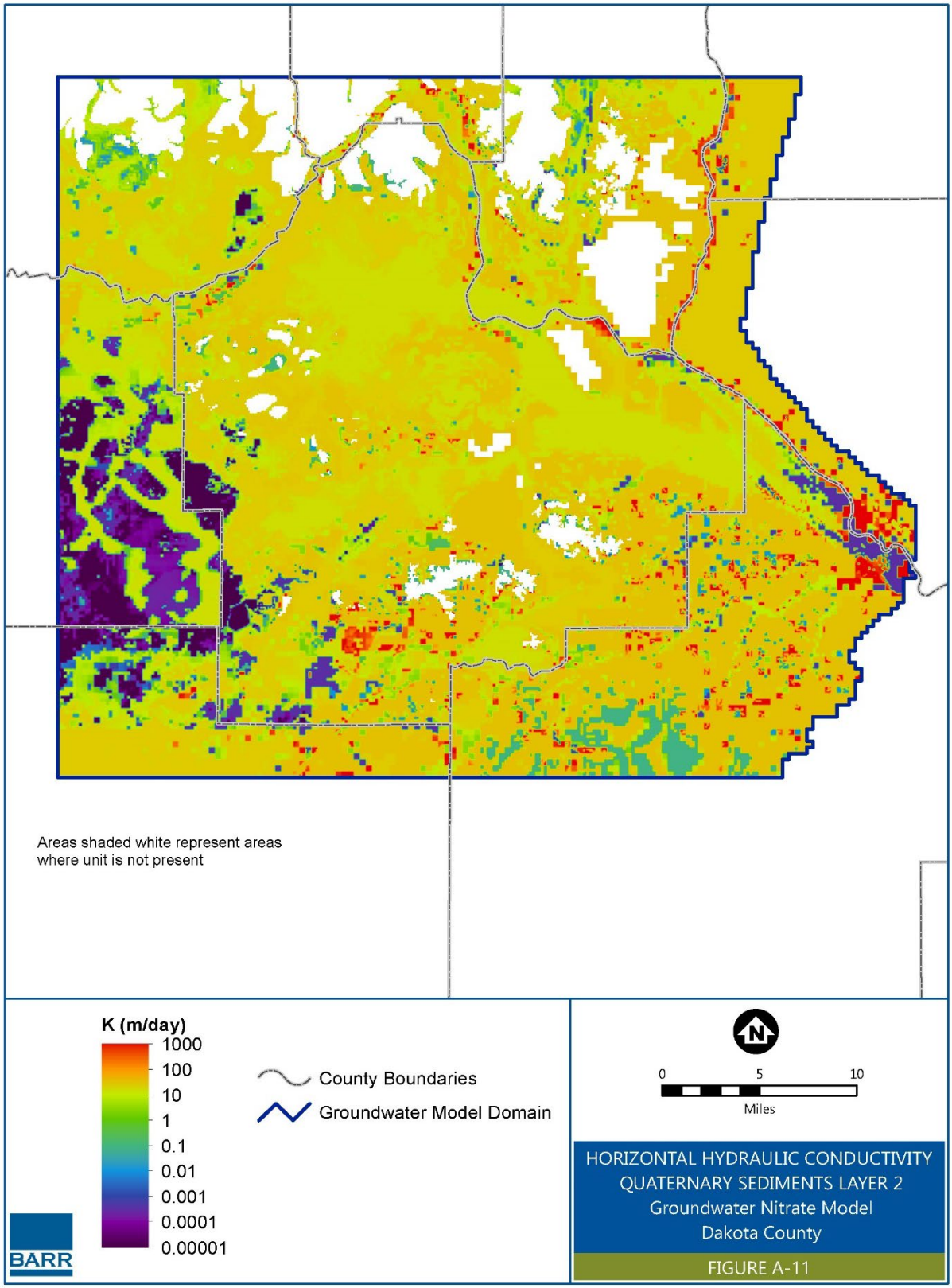

Figure A-12 Vertical Hydraulic Conductivity: Quaternary Sediments Layer 2

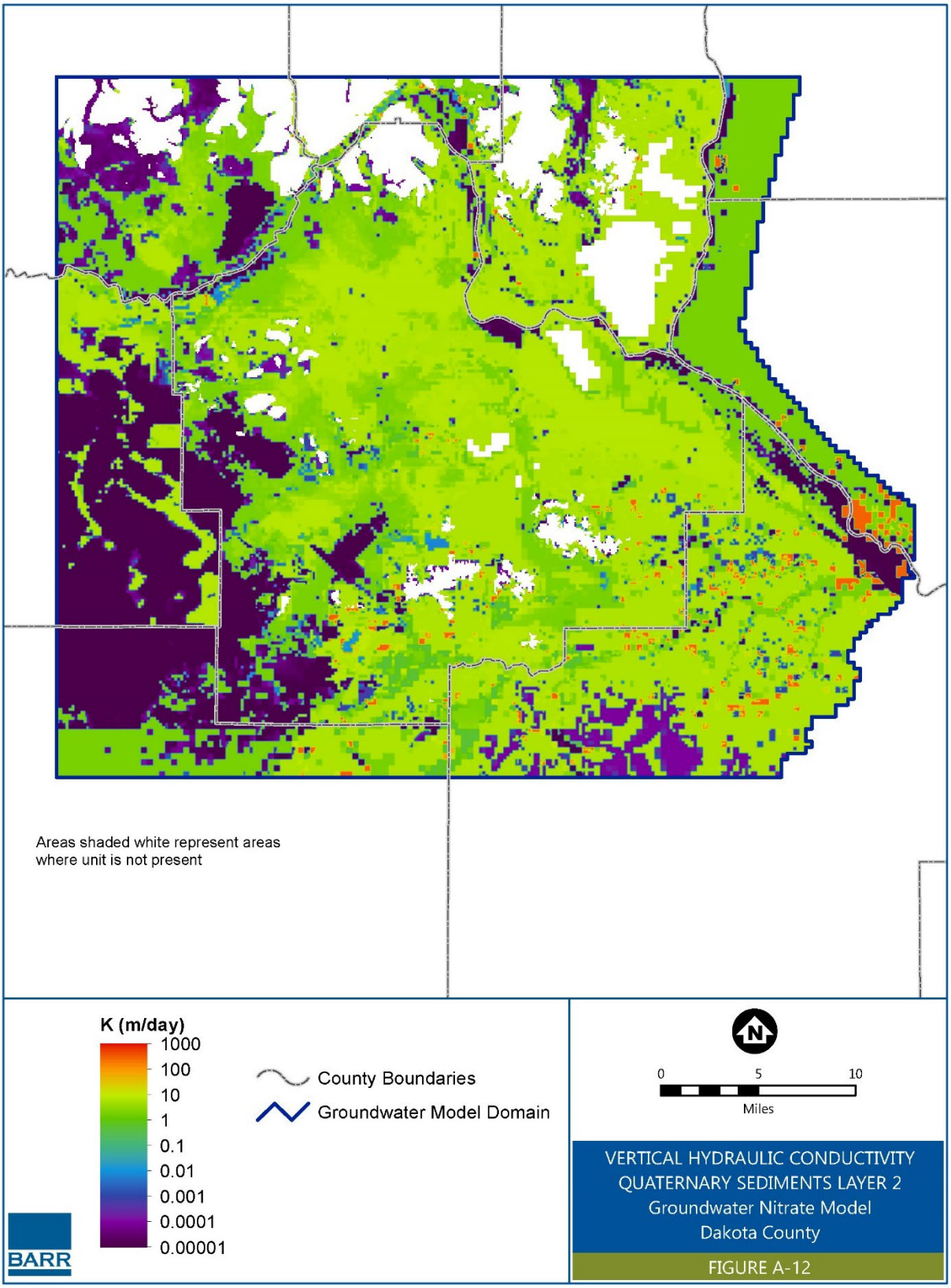

Figure A-13 Horizontal Hydraulic Conductivity: Quaternary Sediments Layer 3

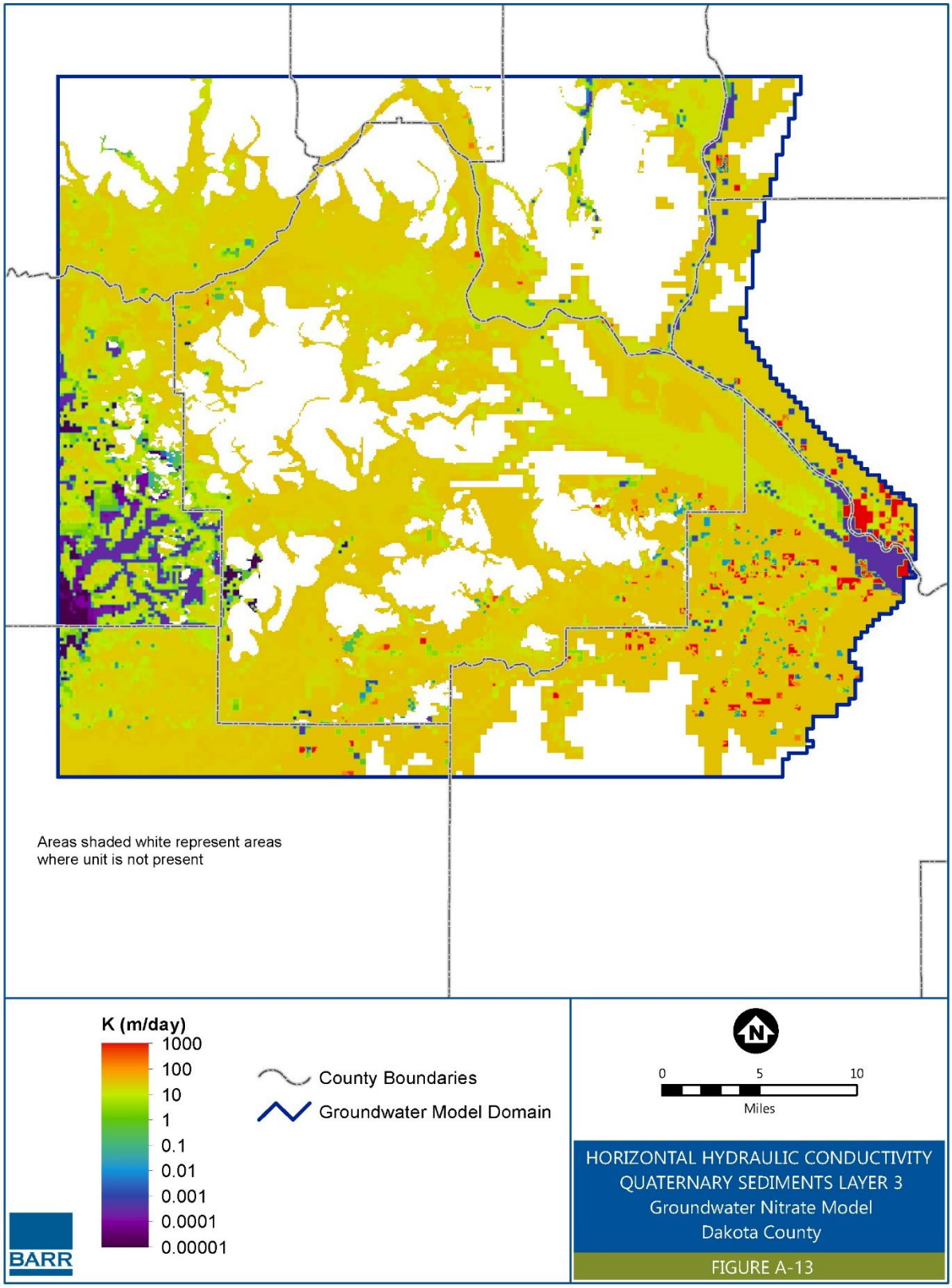

Figure A-14 Vertical Hydraulic Conductivity: Quaternary Sediments Layer 3

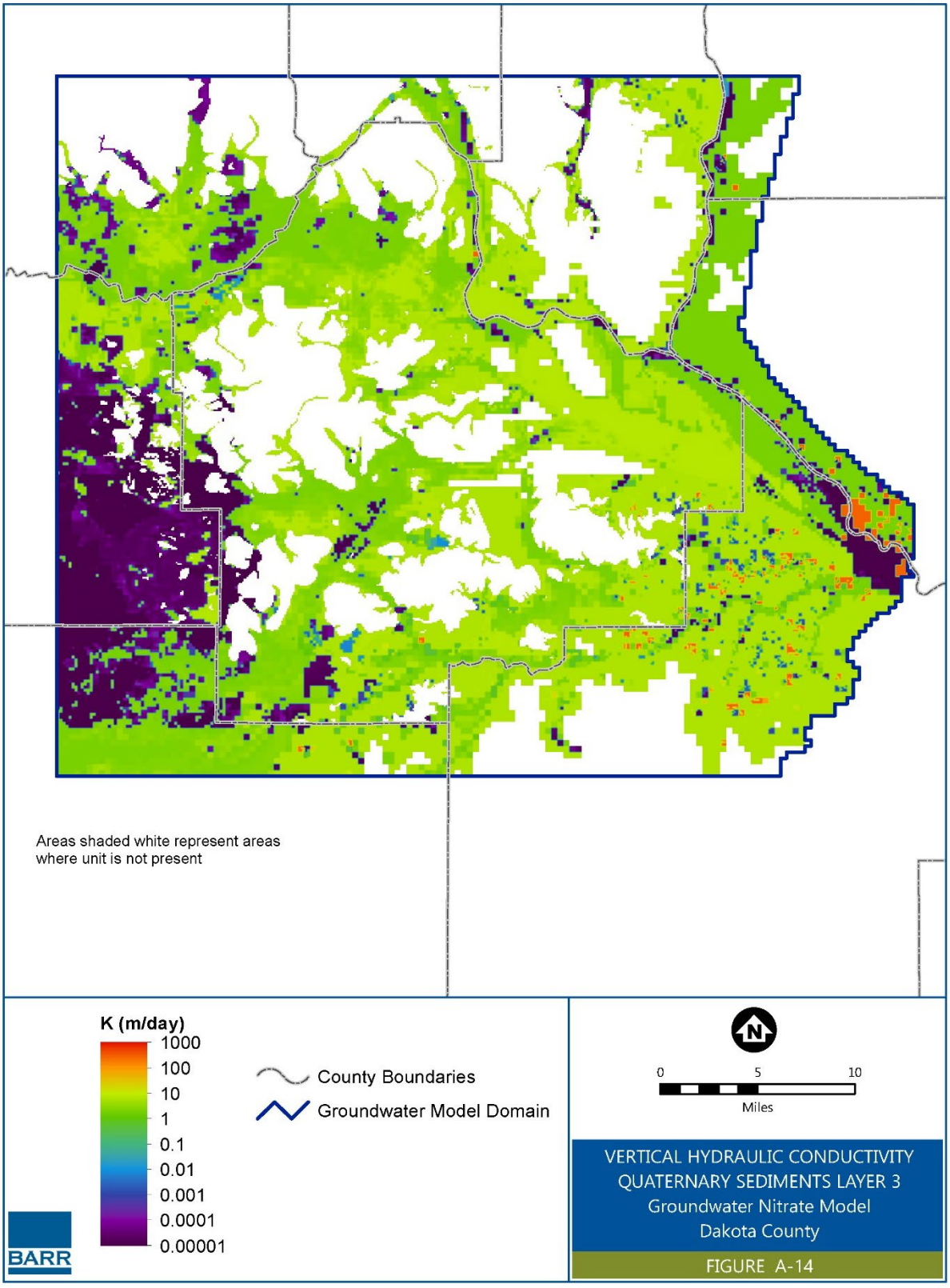

Figure A-15 Horizontal Hydraulic Conductivity: Quaternary Sediments Layer 4

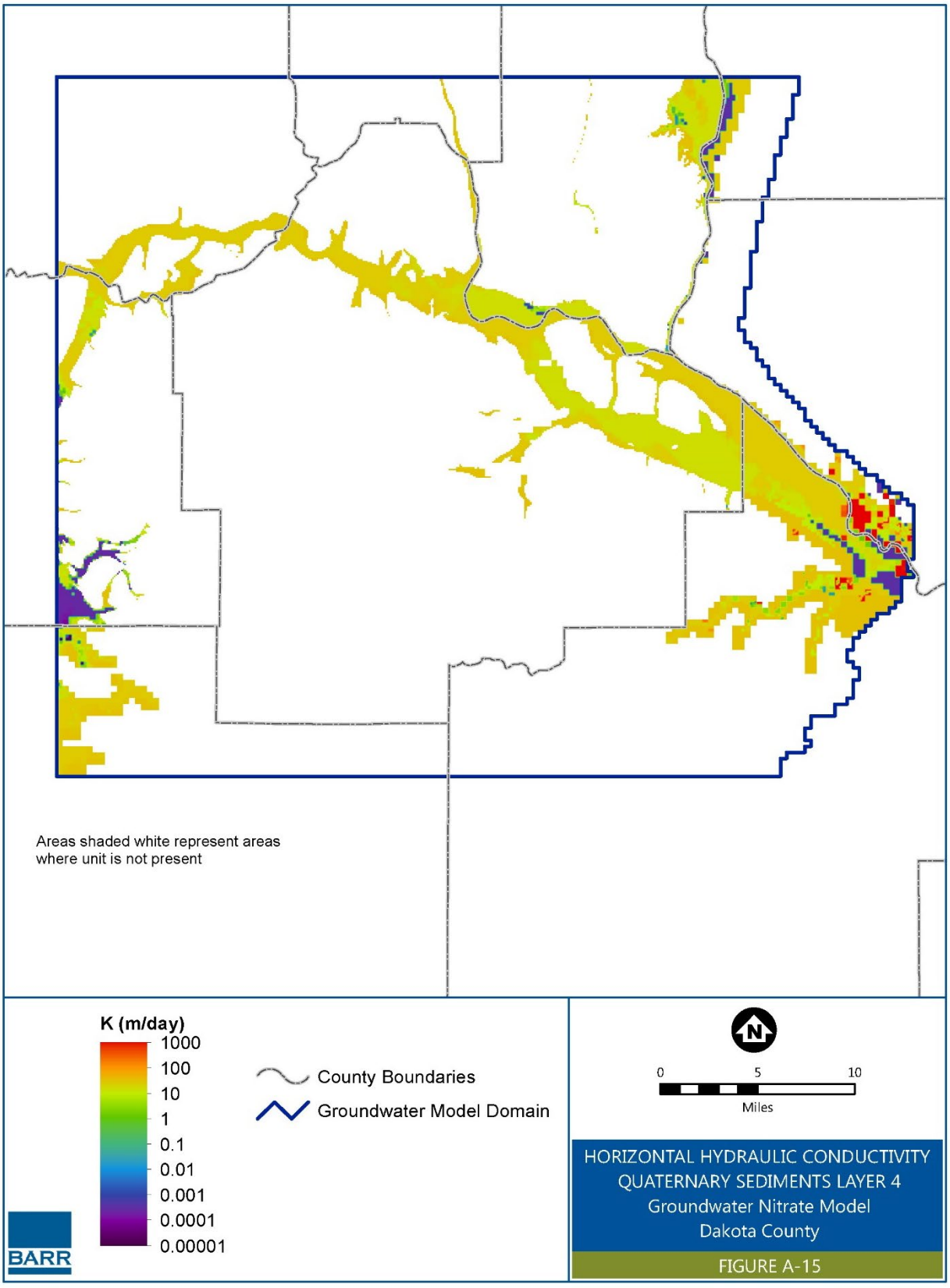

Figure A-16 Vertical Hydraulic Conductivity: Quaternary Sediments Layer 4

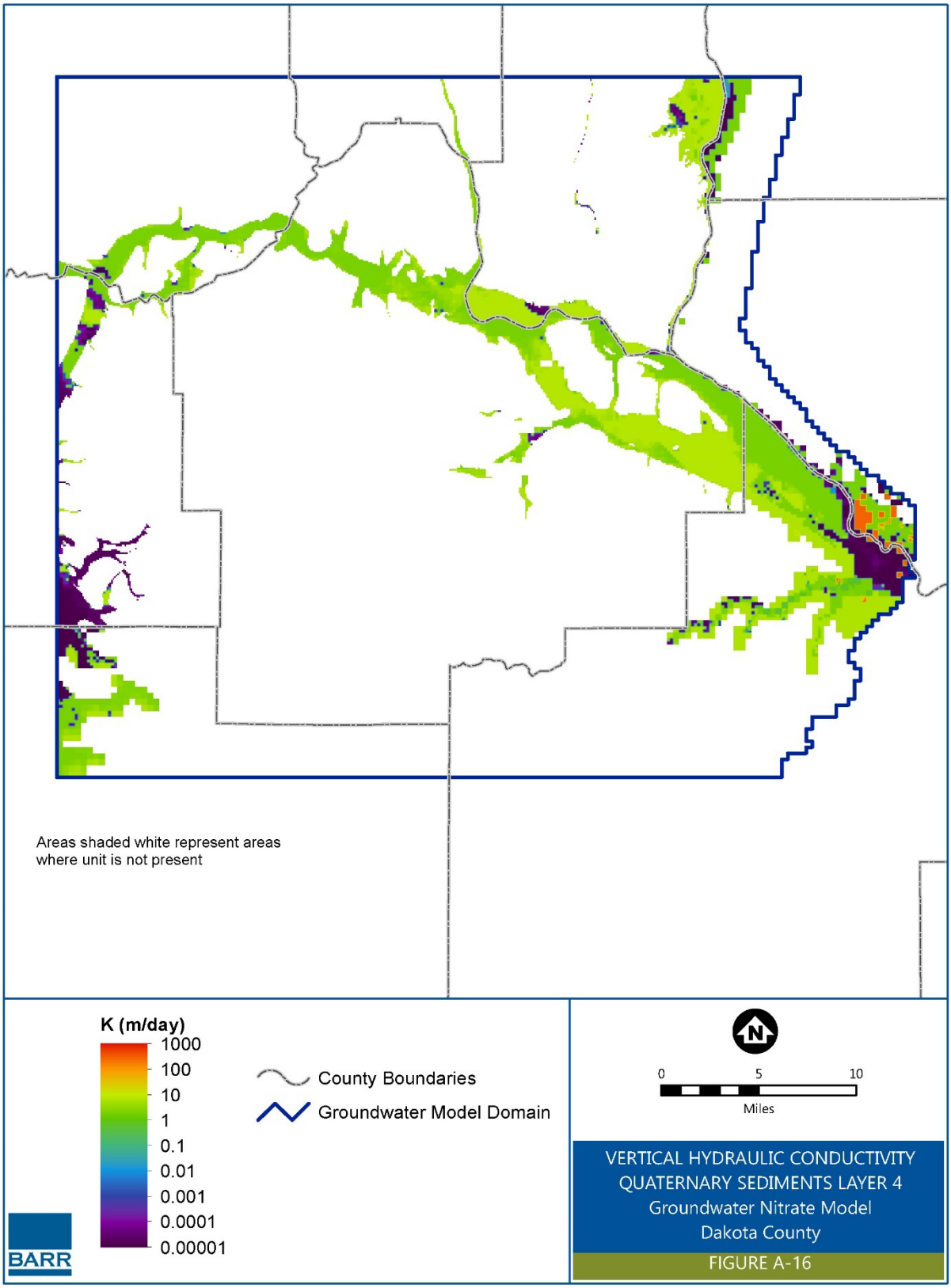

Figure A-17 Horizontal Hydraulic Conductivity: Quaternary Sediments Layer 5

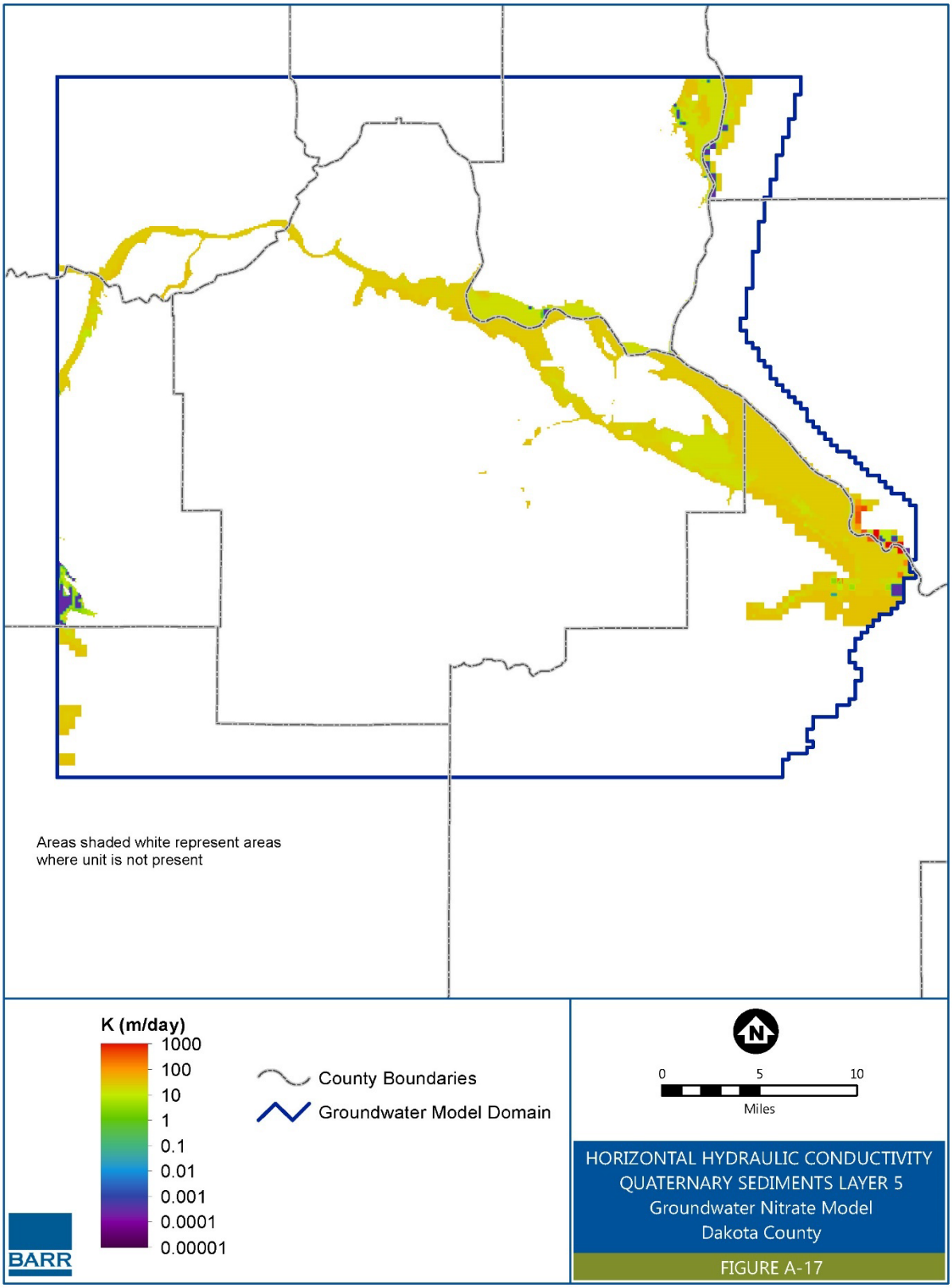

Figure A-18 Vertical Hydraulic Conductivity: Quaternary Sediments Layer 5

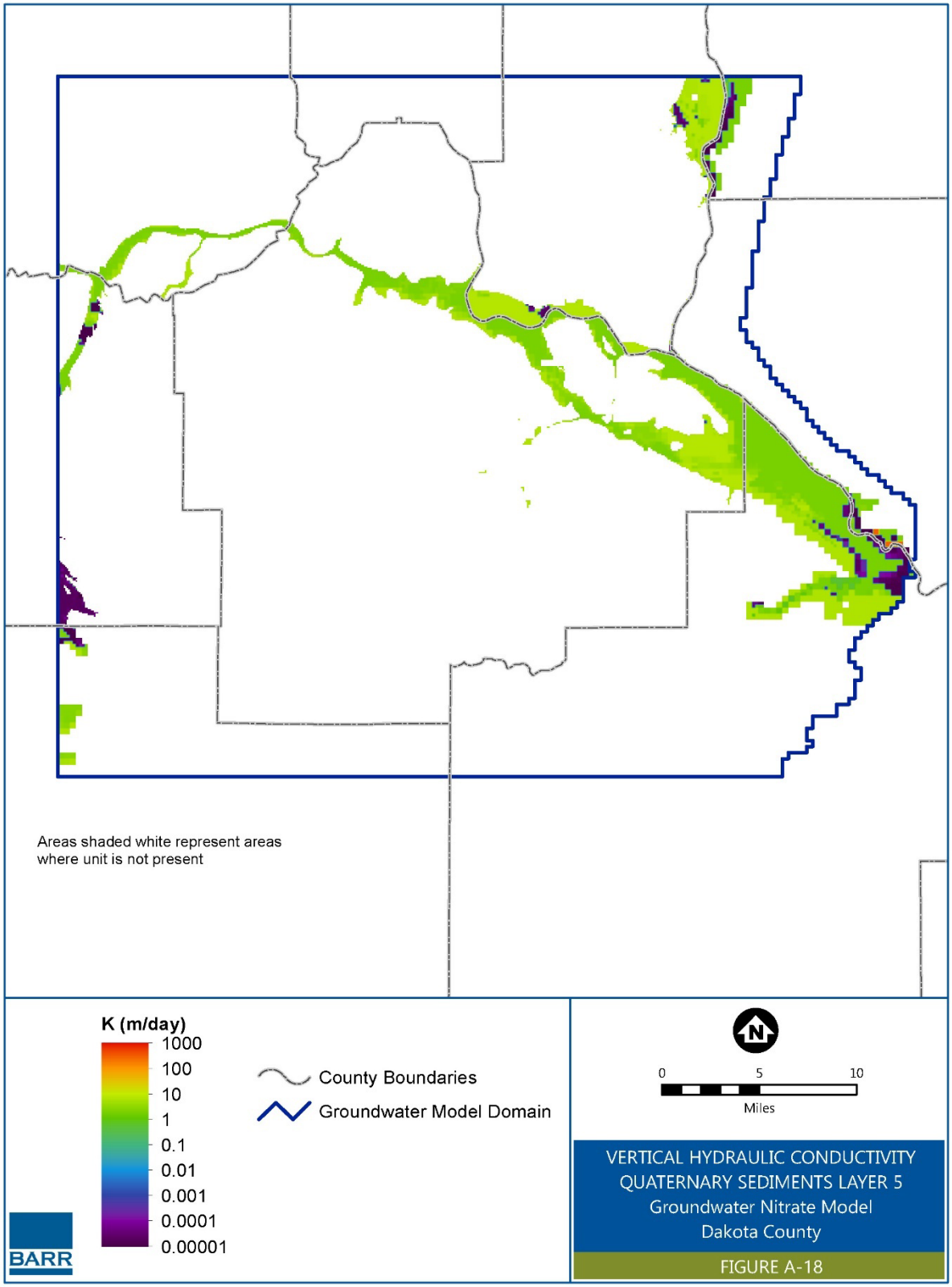

Figure A-19 Precipitation-Derived Infiltration